Coordination Chemistry Reviews 255 (2011) 899–919

Contents lists available at ScienceDirect

Coordination Chemistry Reviews

journal homepage: www.elsevier.com/locate/ccr

Review

Ruthenium complexes of 1,4,7-trimethyl-1,4,7-triazacyclononane for atom and group transfer reactions

Sharon Lai-Fung Chan, Yu-He Kan, Ka-Lai Yip, Jie-Sheng Huang, Chi-Ming Che*

Department of Chemistry and State Key Laboratory on Synthetic Chemistry, The University of Hong Kong, Pokfulam Road, Hong Kong

Contents

ARTICLE INFO

Article history:
Received 4 September 2010
Accepted 17 November 2010
Available online 25 November 2010

Dedicated to Professor Harry B. Gray on the occasion of his 75th birthday.

Keywords:
Ruthenium
1,4,7-Trimethyl-1,4,7-triazacyclononane (Me_3tacn)
Ruthenium-oxo and -imido complexes

ABSTRACT

With support by macrocyclic tertiary amine ligand 1,4,7-trimethyl-1,4,7-triazacyclononane (Me_3tacn), a number of mononuclear metal–ligand multiple bonded complexes have been isolated. Starting with a brief summary of these complexes, the present review focuses on ruthenium-oxo and -imido complexes of Me_3tacn. A family of monooxoruthenium(IV) complexes $[Ru^{IV}(Me_3tacn)O(N–N)]^{2+}$ (N–N = 2,2′-bipyridines) and a *cis*-dioxoruthenium(VI) complex *cis*-$[Ru^{VI}(Me_3tacn)O_2(CF_3CO_2)]^+$ have been isolated, and the structures of $[Ru^{IV}(Me_3tacn)O(bpy)](ClO_4)_2$ (bpy = 2,2′-bipyridine) and *cis*-$[Ru^{VI}(Me_3tacn)O_2(CF_3CO_2)]ClO_4$ have been determined by X-ray crystallography. Oxidation of $[Ru^{III}(Me_3tacn)(NHTs)_2(OH)]$ (Ts = *p*-toluenesulfonyl) with Ag^+ and electrochemical oxidation of $[Ru^{III}(Me_3tacn)(H_2L)](ClO_4)_2$ (H_3L = α-(1-amino-1-methylethyl)-2-pyridinemethanol) are likely to generate ruthenium-imido complexes supported by Me_3tacn. DFT calculations on *cis*-$[Ru^{VI}(Me_3tacn)O_2(CF_3CO_2)]^+$ and proposed ruthenium-imido complexes have been performed. Complexes $[Ru^{IV}(Me_3tacn)O(N–N)]^{2+}$ are reactive toward alkene epoxidation, and *cis*-$[Ru^{VI}(Me_3tacn)O_2(CF_3CO_2)]^+$ efficiently oxidizes various organic substrates including concerted [3+2]

* Corresponding author. Tel.: +852 28592154; fax: +852 28571586.
E-mail address: cmche@hku.hk (C.-M. Che).

0010-8545/$ – see front matter © 2010 Elsevier B.V. All rights reserved.
doi:10.1016/j.ccr.2010.11.026

cycloaddition reactions with alkynes and alkenes to selectively afford α,β-diketones, *cis*-diols, or C=C bond cleavage products. Related oxidation reactions catalyzed by ruthenium Me_3tacn complexes include epoxidation of alkenes, *cis*-dihydroxylation of alkenes, oxidation of alkanes, alcohols, aldehydes, and arenes, and oxidative cleavage of C≡C, C=C, and C–C bonds, all of which exhibit high selectivity. Ruthenium Me_3tacn complexes are also active catalysts for amination of saturated C–H bonds.

© 2010 Elsevier B.V. All rights reserved.

1. Introduction

Starting from Werner type complexes, amine ligands have been playing and continue to play an important role in the advances of inorganic chemistry. Saturated amines are good σ donor ligands, optically transparent in the UV–visible spectral region and, in the case of tertiary amines, are resistant toward oxidation upon coordination to metal ions. Besides monodentate and bidentate amines that are classic ligand systems in transition metal chemistry, extensive efforts have been made to develop cyclic amine ligands for their strong chelating power to metal ions and for the fact that metal complexes in unusual oxidation states can often be stabilized by using macrocyclic amine ligands [1]. The paper by Bosnich et al. [2] on 1,4,8,11-tetraazacyclotetradecane (14-aneN4) is a seminal work in the field of macrocyclic metal complexes. In the past decades, by using the *N*-methyl derivatives of 14-aneN4 such as TMC (1,4,8,11-tetramethyl-1,4,8,11-tetraazacyclotetradecane) and its analogues, novel transition metal complexes in both low and high oxidation states including the high-valent metal-oxo complexes of ruthenium [3] and iron [4] can be stabilized and prepared. However, the rigid and tetradentate nature of TMC disfavors the formation of metal complexes having two or more reactive sites in a *cis* configuration. In this regard, the ligands 1,4,7-triazacyclononane (tacn) and 1,4,7-trimethyl-1,4,7-triazacyclononane (Me_3tacn), first reported by Koyama and Yoshino [5] and subsequently advanced by Wieghardt et al. [6], have become a landmark ligand system that impacts the development of bioinorganic chemistry and catalysis [7]. As with TMC, Me_3tacn is resistant to oxidation upon metal ion coordination, implying that it is a good ligand for developing robust oxidative catalysts. Importantly, the facial coordination mode of Me_3tacn to metal ions makes it structurally resemble the classic η^5-cyclopentadienyl (Cp) type ligands leaving at least two coordination sites available for substrate binding and activation.

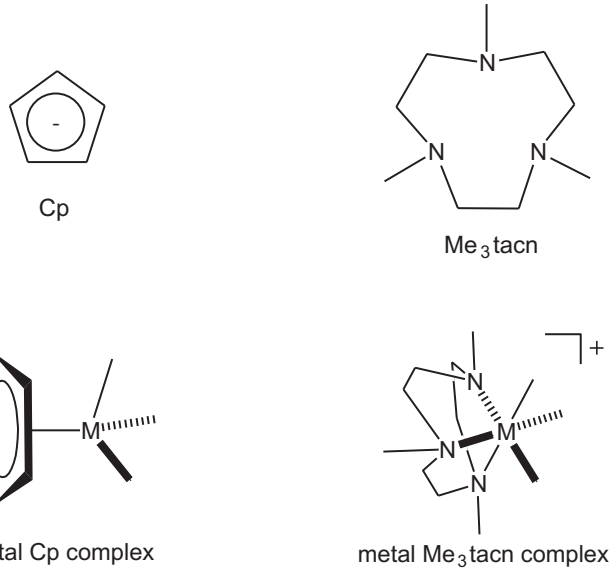

Manganese Me_3tacn complexes such as $[\{Mn(Me_3tacn)\}_2(\mu\text{-}OH)(\mu\text{-}OAc)_2]^{n+}$ (n = 1–3) and $[\{Mn^{IV}(Me_3tacn)\}_2(\mu\text{-}O)_3]^{2+}$, first synthesized and structurally characterized by Wieghardt et al. in 1980s [8], are of particular importance in the development of Me_3tacn-supported transition metal complexes. Studies on these dinuclear manganese complexes by Wieghardt et al. revealed that Me_3tacn is a good ligand system for developing model compounds of manganese-containing biologically important enzymes such as photosynthetic enzymes PSII and pseudocatalase [8]. A seminal report by Hage et al. in 1994 demonstrated that di- and mononuclear manganese complexes of Me_3tacn and related ligands, including $[\{Mn^{IV}(Me_3tacn)\}_2(\mu\text{-}O)_3]^{2+}$, are highly effective catalysts for low temperature bleaching by H_2O_2 and for alkene epoxidation with H_2O_2 [9]. This work subsequently stimulated considerable interest in developing catalytic oxidations using manganese catalysts bearing Me_3tacn or related ligands, including $[\{Mn^{IV}(Me_3tacn)\}_2(\mu\text{-}O)_3]^{2+}$-catalyzed epoxidation of alkenes, *cis*-dihydroxylation of alkenes, and oxidation of C–H bonds and alcohols with H_2O_2, and oxidation of sulfides to sulfones with periodic acid, as described in a recent review [10].

Iron Me_3tacn complexes that exhibit interesting oxidation properties have also been documented, mainly as model systems for nonheme iron enzymes such as hemerythrin, extradiol-cleaving catechol dioxygenase, and methane monooxygenase. Wieghardt and co-workers [11] reported that the unsymmetrical dinuclear complex $[(Me_3tacn)Fe(\mu\text{-}O)(\mu\text{-}O_2CMe)_2Fe(bpy)(OH_2)](ClO_4)_2$ catalyzed disproportionation of H_2O_2 to O_2 and H_2O (a catalase activity). Que and co-worker [12] found that mononuclear complex [Fe(Me_3tacn)(DBC)Cl] (DBC = 3,5-di-*tert*-butylcatecol) reacted with O_2 in the presence of AgOTf to afford extradiol cleavage products of DBC in an excellent yield. By employing dinuclear complexes $[\{Fe(Me_3tacn)\}_2(\mu\text{-}O_2CAr)_2(MeCN)_2](OTf)_2$ or $[\{Fe(Me_3tacn)\}_2(\mu\text{-}O)(\mu\text{-}O_2CAr)_2](OTf)_2$ (O_2CAr = 2,6-di(*p*-tolyl)-benzoate) as catalyst, Lippard and co-workers [13] developed oxygen atom transfer reactions catalyzed by iron Me_3tacn complexes, including aerobic oxidation of PR_3 to O=PR_3 and oxidation of THF to a C–C bond cleavage product.

We are interested to develop multi-electron atom and group transfer catalysis via reactive mononuclear metal Me_3tacn complexes bearing terminal metal–ligand multiple bonds such as metal-oxo (M=O) and -imido (M=NR) complexes, with particular reference to the transition metal ruthenium. Terminal metal–ligand multiple bonded complexes supported by Me_3tacn started to appear in the literature shortly after the first synthesis of this macrocyclic ligand. In 1985 and 1990, Wieghardt et al. reported the characterization of W=O complexes $[W^V(Me_3tacn)OCl_2]^+$ [14] and *cis*-$[W^{VI}(Me_3tacn)O_2(OH)]^+$ [15], respectively, by X-ray crystal analysis. We reported, in 1994, the isolation, crystal structures, and hydrocarbon oxidation reactions of Ru=O complexes $[Ru^{IV}(Me_3tacn)O(bpy)]^{2+}$ [16] and *cis*-$[Ru^{VI}(Me_3tacn)O_2(CF_3CO_2)]^+$ [17]; these two complexes are potent oxidants/catalysts for alkene epoxidation and alkene *cis*-dihydroxylation reactions. Wieghardt and co-workers also synthesized and structurally characterized manganese-nitrido complex $[Mn^V(Me_3tacn)N(acac)]^+$, which was reported in 1996 [18]. Subsequently we reported the syntheses and crystal structures of molybdenum/tungsten-carbyne complexes $[M(Me_3tacn)(CPh)(CO)_2]^+$ (M = Mo, W) in 1998 [19] and chromium-imido complex *cis*-$[Cr^{VI}(tacn)\{N(t\text{-}Bu)\}_2Cl]^+$ (together with the isolation of *cis*-$[Cr^{VI}(Me_3tacn)\{N(t\text{-}Bu)\}_2Cl]^+$) in 1999 [20].

Table 1
Terminal metal–ligand multiple bonded complexes supported by Me_3tacn (selected bond distances and angles for structurally characterized complexes are indicated).

Complex[a]	Bond distance (Å)		Bond angle (°)		Reference
$[Ti^{IV}(Me_3tacn)O(NCS)_2]$	Ti=O	1.638(3)			[25]
$[Ti^{IV}(Me_3tacn)OCl_2]$	Ti=O	1.637(3)			[26]
$[V^{IV}(Me_3tacn)OCl_2]$	V=O	1.637(3)			[27b]
$[Mn^{IV}(Me_3tacn)O(OH_2)]^{2+}$					[22]
$[Mo^{IV}(Me_3tacn)OI_2]$					[28]
$[Mo^{V}(Me_3tacn)OX_2]^+$ (X = Cl, Br, I)					[29]
$[Mo^{V}(Me_3tacn)O(OMe)_2]^+$					[28]
cis-$[Mo^{VI}(Me_3tacn)O_2Br]^+$					[29]
cis-$[Mo^{VI}(Me_3tacn)O_2(OMe)]^+$	Mo=O	1.705(1)	O=Mo=O	105.7(1)	[30]
cis-$[Mo^{VI}(Me_3tacn)O_2\{OSi(i\text{-}Pr)_3\}]^+$	Mo=O	1.700(1)	O=Mo=O	105.9(1)	[30]
cis-$[Mo(Me_3tacn)O_2\{OB(C_6F_5)_3\}]$					[31]
$[Mo^{VI}(Me_3tacn)O_3]$					[32]
$[Ru^{IV}(Me_3tacn)O(bpy)]^{2+}$	Ru=O	1.815(6)			[16]
$[Ru^{IV}(Me_3tacn)O(3,3'\text{-}Me_2bpy)]^{2+}$					[33]
$[Ru^{IV}(Me_3tacn)O(cbpy^*)]^{2+}$					[33]
$[Ru^{IV}(Me_3tacn)O(biqn)]^{2+}$					[34]
$[Ru^{IV}(Me_3tacn)O(diopy^*)]^{2+}$					[34]
cis-$[Ru^{VI}(Me_3tacn)O_2(CF_3CO_2)]^+$	Ru=O	1.716(9)[b]	O=Ru=O	118.3(4)	[17]
$[W^{V}(Me_3tacn)OCl_2]^+$	W=O	1.719(18)			[14]
$[W^{V}(Me_3tacn)OX_2]^+$ (X = F, Br)					[35]
cis-$[W^{VI}(Me_3tacn)O_2X]^+$ (X = F, Cl, Br)					[35]
cis-$[W^{VI}(Me_3tacn)O_2(OMe)]^+$					[30]
cis-$[W^{VI}(Me_3tacn)O_2\{OSi(i\text{-}Pr)_3\}]^+$	W=O	1.719(1)	O=W=O	105.7(1)	[30]
cis-$[W(Me_3tacn)O_2\{OB(C_6F_5)_3\}]$	W=O	1.714(3)[b]	O=W=O	106.7(2)	[31]
cis-$[W^{VI}(Me_3tacn)O_2(OH)]^+$	W=O	1.78(2)[b]	O=W=O	110.6(9)	[15]
$[W^{VI}(Me_3tacn)O_3]$					[32]
$[Re^{V}(Me_3tacn)OCl_2]^+$					[36]
$[Re^{V}(Me_3tacn)O(OMe)_2]^+$					[37]
cis-$[Re^{V}(Me_3tacn)O_2(OH_2)]^+$	Re=O	1.80(1)[b]	O=Re=O	106.7(5)	[39]
$[Re^{VII}(Me_3tacn)O_3]^+$	Re=O	1.716(2)[b]	O=Re=O	105.8(1)[b]	[38]
$[Ti(Me_3tacn)\{N(t\text{-}Bu)\}Cl_2]$	Ti=N	1.699(4)	Ti=N–C	176.3(4)	[40]
$[Ti(Me_3tacn)\{N(t\text{-}Bu)\}(CH_2Ph)_2]$	Ti=N	1.713(3)	Ti=N–C	176.8(3)	[40]
$[Ti(Me_3tacn)\{N(p\text{-}MeC_6H_4)\}Cl_2]$					[40]
$[Ti(Me_3tacn)\{N(2,6\text{-}(i\text{-}Pr)_2C_6H_3)\}Cl_2]$					[40]
$[Ti(Me_3tacn)(NNPh_2)Cl_2]$					[41]
cis-$[Cr^{VI}(Me_3tacn)\{N(t\text{-}Bu)\}_2Cl]^+$					[20]
cis-$[Mo(Me_3tacn)\{N(t\text{-}Bu)\}_2Cl]^+$					[20]
$[Ru(Me_3tacn)(C{=}CHPh)(PMe_3)(CF_3CO_2)]^+$					[42]
$[Ru(Me_3tacn)\{C{=}CH(p\text{-}MeC_6H_4)\}(PMe_3)(CF_3CO_2)]^+$					[42]
$[Ru(Me_3tacn)\{C(OMe)CH_2Ph\}(phen)]^{2+}$	Ru=C	1.917(3)	Ru=C–C	126.3(2)	[43]
$[Ru(Me_3tacn)\{C(OMe)CH{=}CPh_2\}(phen)]^{2+}$	Ru=C	1.906(4)	Ru=C–C	123.1(3)	[43]
$[Ru(Me_3tacn)\{C{=}C{=}CPh_2\}(phen)]^{2+}$					[43]
$[Mn^{V}(Me_3tacn)N(acac)]^+$	Mn≡N	1.518(4)			[18]
$[Mn^{V}(Me_3tacn)N(N_3)_2]$					[44]
$[Mo(Me_3tacn)(CPh)(CO)_2]^+$	Mo≡C	1.797(6)	Mo≡C–C	174.7(5)	[19]
$[W(Me_3tacn)(CPh)(CO)_2]^+$	W≡C	1.800(6)	W≡C–C	174.4(4)	[19]

[a] acac, pentane-2,4-dionate; biqn, 1,1′-biisoquinoline; bpy, 2,2′-bipyridine; cbpy*, (−)-3,3′-[(4*S*-*trans*)-1,3-dioxolane-4,5-dimethyl]-2,2′-bipyridine; diopy*, (*R*,*R*′)-3,3′-(1,2-dimethylethylenedioxy)-2,2′-bipyridine; 3,3′-Me_2bpy, 3,3′-dimethyl-2,2′-bipyridine; phen, 1,10-phenanthroline.
[b] Mean value.

In some cases the oxidation reactions catalyzed by manganese Me_3tacn complexes were proposed to involve high-valent Mn^{IV}=O or Mn^{V}=O as reaction intermediates [10], but so far there have been no reports on structurally characterized terminal Mn=O complexes supported by Me_3tacn. Lindsay Smith and co-workers reported detection of $[Mn^{V}(Me_3tacn)O(biphenol)]^+$ by ESI mass spectrometry [21], and the isolation and spectroscopic characterization of $[Mn^{IV}(Me_3tacn)O(OH_2)]SO_4$ were subsequently reported by Srinivas and co-workers [22]. In the case of iron, isolation of its Me_3tacn complexes bearing terminal Fe=O bonds has not been documented. Halfen and co-workers [23] recently reported the aziridination of alkenes with PhI=NR (R = *p*-toluenesulfonyl) catalyzed by $[Fe^{II}(i\text{-}Pr_3tacn)(CF_3SO_3)_2]$ (*i*-Pr_3tacn = 1,4,7-tri(isopropyl)-1,4,7-triazacyclononane), which is proposed to involve Fe^{IV}=NR species [24]. Besides W, Ru, Mo, Cr, and Mn, other transition metals, such as Ti, V, and Re, are known to form isolable complexes with Me_3tacn bearing metal–ligand multiple bonds. A summary of the isolated mononuclear terminal metal–ligand multiple bonded complexes supported by Me_3tacn, including metal-oxo [14–17,22,25–39], -imido [20,40,41], -carbene/-vinylidene/-allenylidene [42,43], -nitrido [18,44], and -carbyne [19] complexes, is depicted in Table 1.

In this review, we focus on the Me_3tacn complexes of ruthenium bearing terminal ruthenium-ligand multiple bonds including ruthenium-oxo and -imido species and their oxygen [16,17,33,34,45–47] and nitrogen atom/group transfer reactions, together with related reactions catalyzed by ruthenium Me_3tacn complexes, including epoxidation of alkenes [17,48,49], oxidation of alkanes [17,48], alcohols [50,51], aldehydes [51], and arenes [52], oxidative cleavage of C=C, C≡C, and C–C bonds [51], *cis*-dihydroxylation of alkenes [53], and amination of saturated C–H bonds [54]. Also included here are some of our unpublished results on the DFT calculations on reactive Ru=O and Ru=NTs (Ts = *p*-toluenesulfonyl) complexes supported by Me_3tacn, and on C–N bond formation reactions catalyzed by $[Ru(Me_3tacn)(NH_3)_3]^{2+}$, and electrochemical oxidation of Ru(III)–NH_2R to the putative

$[Ru^{V}{=}NR]^{2+}$ from the $[Ru(Me_3tacn)(H_2L)]^{2+}$ (H_3L = α-(1-amino-1-methylethyl)-2-pyridinemethanol) complex [55].

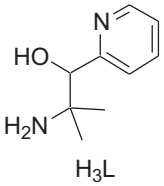

2. Monooxoruthenium(IV) complexes

Ruthenium complexes of Me_3tacn were first reported by Wieghardt and co-workers in 1988 [56]; these earliest examples include $[Ru^{III}(Me_3tacn)Cl_3]$, $[\{Ru^{III}(Me_3tacn)\}_2(\mu\text{-}O)(\mu\text{-}OAc)_2](PF_6)_2$, $[\{Ru^{III}(Me_3tacn)\}_2(\mu\text{-}OH)(\mu\text{-}OAc)_2](PF_6)_3$, and $[(Me_3tacn)Ru^{III}(\mu\text{-}O)(\mu\text{-}OAc)_2Ru^{IV}(Me_3tacn)](PF_6)_3$, of which the two μ-O complexes are structurally characterized by X-ray crystal analysis.

2.1. Synthesis and characterization

In 1993, Wieghardt and co-workers proposed the formation of $[Ru^{IV}(Me_3tacn)O(acac)]^+$ upon electrochemical oxidation of $[Ru^{III}(Me_3tacn)(OH)(acac)]^+$ in MeCN; attempts to isolate this Ru=O species through chemical oxidation were not successful [57]. Since 1994, we reported a family of $[Ru^{IV}(Me_3tacn)O(N\text{–}N)]^{2+}$ (N–N = 2,2′-bipyridines) complexes isolated as ClO_4^- or PF_6^- salts, including $[Ru^{IV}(Me_3tacn)O(bpy)](ClO_4)_2$ [16], $[Ru^{IV}(Me_3tacn)O(3,3'\text{-}Me_2bpy)](ClO_4)_2$ [33], $[Ru^{IV}(Me_3tacn)O(cbpy^*)](PF_6)_2$ [33], $[Ru^{IV}(Me_3tacn)O(biqn)](ClO_4)_2$ [34], and $[Ru^{IV}(Me_3tacn)O(diopy^*)](ClO_4)_2$ [34], in which cbpy* and diopy* are chiral 2,2′-bipyridine derivatives. These Ru=O complexes were prepared through reactions of $[Ru^{III}(Me_3tacn)Cl_3]$ with the corresponding N–N ligand in the presence of Zn powder in water to give $[Ru^{II}(Me_3tacn)(N\text{–}N)Cl]^+$, which upon removal of Cl^- by Ag(I) led to $[Ru^{II}(Me_3tacn)(OH_2)(N\text{–}N)]^{2+}$, followed by oxidation with $(NH_4)_2[Ce^{IV}(NO_3)_6]$ in water (Scheme 1). The X-ray crystal structure of $[Ru^{IV}(Me_3tacn)O(bpy)](ClO_4)_2$ (Fig. 1) shows the Ru=O distance of 1.815(6) Å [16]. All of the $[Ru^{IV}(Me_3tacn)O(N\text{–}N)]^{2+}$ complexes are paramagnetic with $S = 1$ ground state [$\mu_{eff} = 2.83\ \mu_B$ for $[Ru^{IV}(Me_3tacn)O(bpy)](ClO_4)_2$]. Their ν(Ru=O) stretching frequencies are in the range of 779–796 cm^{-1}.

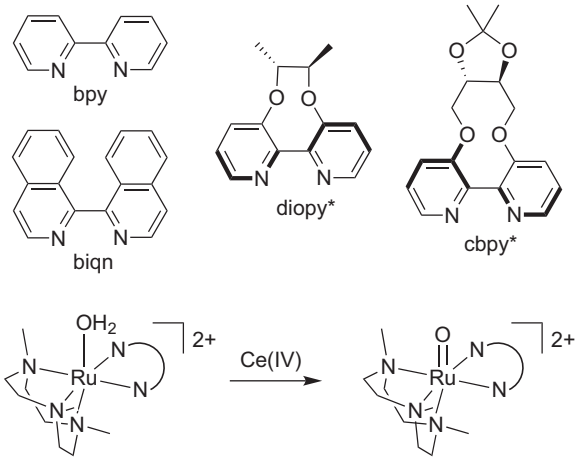

Scheme 1.

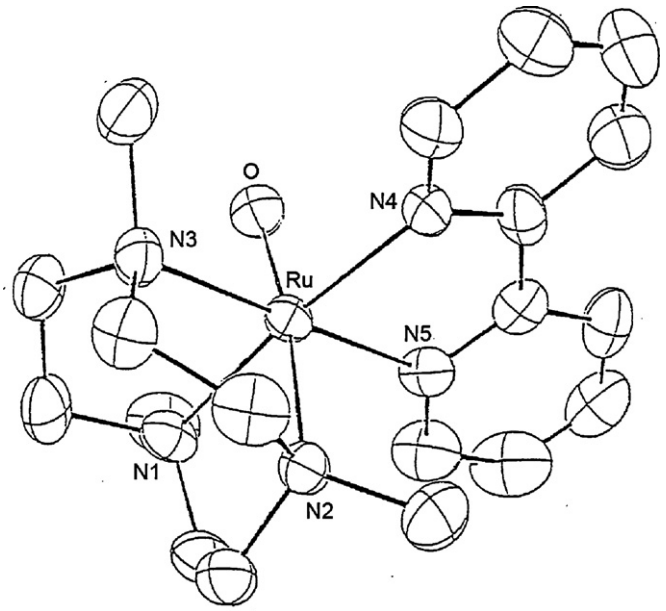

Fig. 1. Structure of $[Ru^{IV}(Me_3tacn)O(bpy)](ClO_4)_2$ with omission of hydrogen atoms and perchlorate ion [16].

In aqueous solutions, reversible/quasi-reversible proton-coupled electron transfer redox couples have been observed for $[Ru^{IV}(Me_3tacn)O(N\text{–}N)]^{2+}$ with $E_{1/2}$ of Ru(IV)/Ru(III) couple being 0.90 V vs. SCE for $[Ru^{IV}(Me_3tacn)O(bpy)]^{2+}$ at pH 1.0. A typical cyclic voltammogram revealing the two redox couples for electrochemical oxidation of $[Ru^{II}(Me_3tacn)(OH_2)(bpy)]^{2+}$ to $[Ru^{IV}(Me_3tacn)O(bpy)]^{2+}$ is depicted in Fig. 2 [58].

2.2. Epoxidation reactions with alkenes

The isolated monooxoruthenium(IV) complexes are competent oxidants which can effect alkene epoxidation (Scheme 2) and oxidation of aromatic and allylic C–H bonds at room temperature. $[Ru^{IV}(Me_3tacn)O(bpy)](ClO_4)_2$ reacted with norbornene to give the exo isomer of the epoxide in 79% yield; the same complex oxidized styrene to styrene oxide in 62% yield [45]. For the reaction of $[Ru^{IV}(Me_3tacn)O(biqn)](ClO_4)_2$ with norbornene, the *exo* epoxide was formed in 69% yield [34]. Stoichiometric asymmetric alkene epoxidation by $[Ru^{IV}(Me_3tacn)O(diopy^*)](ClO_4)_2$ has been observed though the enantioselectivity was low, say, *trans*-(1*R*,2*R*)-stilbene oxide was generated in 33% ee from the oxidation of *trans*-stilbene [34]. The reaction of $[Ru^{IV}(Me_3tacn)O(cbpy^*)](PF_6)_2$ with norbornene converted the Ru=O complex to $[Ru^{II}(Me_3tacn)(cbpy^*)(MeCN)]^{2+}$, with the *exo* epoxide of norbornene being obtained in 92% yield [33].

3. *cis*-Dioxoruthenium(VI) complex

Tremendous efforts have been devoted to develop efficient oxidative catalysis using Ru=O complexes of Me_3tacn as catalysts. The $[Ru^{IV}(Me_3tacn)O(N\text{–}N)]^{2+}$ system, even with N–N = 4,4′-dichloro-2,2′-bipyridine, is not sufficiently reactive toward oxidation of unactivated hydrocarbons and aliphatic terminal alkenes. A *cis*-dioxoruthenium complex of Me_3tacn has been prepared.

3.1. Synthesis and characterization

Reaction of $[Ru^{III}(Me_3tacn)Cl_3]$ with AgOTf in neat CF_3CO_2H gave $[Ru^{III}(Me_3tacn)(OH_2)(CF_3CO_2)_2]^+$, which upon oxidation

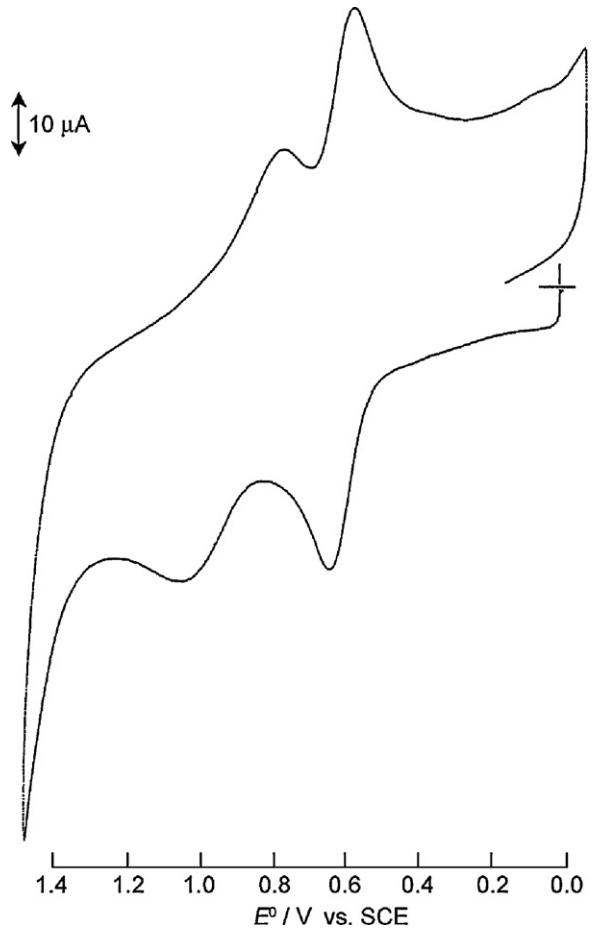

Fig. 2. Cyclic voltammogram of $[Ru^{II}(Me_3tacn)(OH_2)(bpy)](ClO_4)_2$ in 0.1 mol dm^{-3} CF_3CO_2H at scan rate = 100 mV s^{-1} [58].

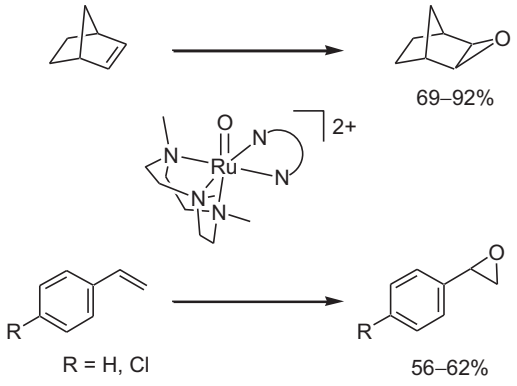

Scheme 2.

by $[NH_4]_2[Ce(NO_3)_6]$ in 0.2 mol dm^{-3} CF_3CO_2H, gave *cis*-$[Ru^{VI}(Me_3tacn)O_2(CF_3CO_2)]^+$ [17] (Scheme 3) isolated as a ClO_4^- salt. *cis*-$[Ru^{VI}(Me_3tacn)O_2(CF_3CO_2)]ClO_4$ is a diamagnetic pale green solid. As expected for *cis*-dioxometal complexes, there are

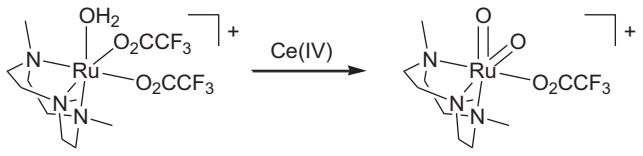

Scheme 3.

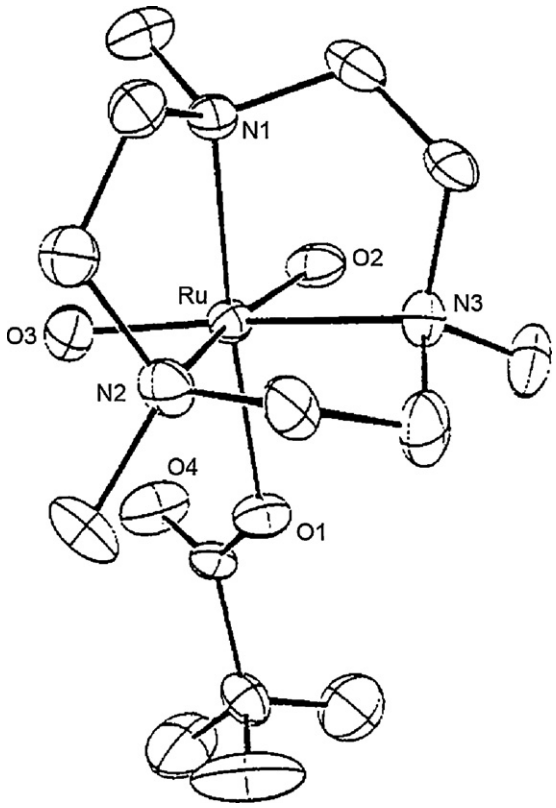

Fig. 3. Structure of $[Ru^{VI}(Me_3tacn)O_2(CF_3CO_2)]ClO_4$ with omission of hydrogen atoms and perchlorate ion [17].

two Ru=O stretching frequencies of 842 and 856 cm^{-1} attributed to the asymmetric and symmetric RuO_2 stretches, respectively. The crystal structure of *cis*-$[Ru^{VI}(Me_3tacn)O_2(CF_3CO_2)]ClO_4$ has been determined [17]. As depicted in Fig. 3, the octahedral geometry of Ru(VI) is fulfilled by the η^3-facially coordinated Me_3tacn ligand with Ru–N distances of 2.097(9)–2.23(2) Å, two oxo ligands with Ru=O distances of 1.717(9) and 1.715(9) Å, and an η^1-trifluoroacetate ligand with Ru–O distance of 2.0467(7) Å. The two oxo ligands are in a *cis*-configuration with O–Ru–O angle of 118.3(4)°.

cis-$[Ru^{VI}(Me_3tacn)O_2(CF_3CO_2)]ClO_4$ is a powerful oxidant. In aqueous solutions, it displays reversible/quasi-reversible proton-coupled electron transfer redox couples. At pH 1.0, the E^o value of Ru(VI)/Ru(V) couple of *cis*-$[Ru^{VI}(Me_3tacn)O_2(CF_3CO_2)]^+$ is 1.1 V vs. SCE, revealing that this complex is thermodynamically capable of oxidizing chloride to chlorine. A typical cyclic voltammogram of *cis*-$[Ru^{VI}(Me_3tacn)O_2(CF_3CO_2)]^+$ is given in Fig. 4 [58]. As revealed from this figure, three reversible/quasi-reversible couples at 1.01 V, 0.9 V, and 0.14 V vs. SCE are observed. To investigate the number of electrons involved in the electrochemical reactions, constant potential coulometry was performed at 0.8 V and 0.1 V, respectively for couples I, II and couple III. The three-electron reduction observed for couples I–II altogether is attributed to the reduction from Ru(VI) to Ru(III). Couple III involves one electron reduction from Ru(III) to Ru(II). As expected for proton-coupled electron transfer reactions, there is a cathodic shift in $E_{1/2}$ values with increase in pH for all of these redox couples.

3.2. DFT calculations

UV–vis absorption spectrum of *cis*-$[Ru^{VI}(Me_3tacn)O_2(CF_3CO_2)]ClO_4$ in 0.1 mol dm^{-3} CF_3CO_2H displays an intense absorption peak at 329 nm

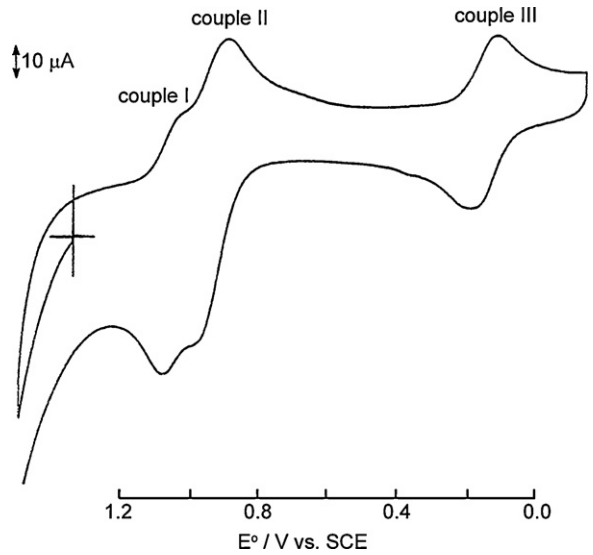

Fig. 4. Cyclic voltammogram of *cis*-$[Ru^{VI}(Me_3tacn)O_2(CF_3CO_2)]^+$ in 0.1 mol dm^{-3} CF_3CO_2H at scan rate = 50 mV s^{-1} [58].

(ε_{max} = 2400 dm^3 mol^{-1} cm^{-1}) and a weak absorption peak at 695 nm ($\varepsilon_{max} \approx 50$ dm^3 mol^{-1} cm^{-1}) (Fig. 5). Time-dependent density functional theory (TD-DFT) is employed to understand the origin of the absorption spectrum (see Appendix for computational details). The X-ray crystal structure of *cis*-$[Ru^{VI}(Me_3tacn)O_2(CF_3CO_2)]^+$ was optimized using Gaussian 03, and TD-DFT studies of *cis*-$[Ru^{VI}(Me_3tacn)O_2(CF_3CO_2)]^+$ were performed using ADF. The optimized bond distances and bond angles of the *cis*-dioxoruthenium(VI) complex using PBE0/SDD/6-31G* are listed in Table 2.

In agreement with the experimental diamagnetic nature of *cis*-$[Ru^{VI}(Me_3tacn)O_2(CF_3CO_2)]^+$, the computed ground state is a singlet. The calculated Ru–N distances are longer by as much as 0.089 Å compared with the experimental data of *cis*-$[Ru^{VI}(Me_3tacn)O_2(CF_3CO_2)]ClO_4$ [17]. Such a large discrepancy has also been experienced in our previous calculation on *trans*-$[Os^{VI}O_2(amine)_4]^{2+}$ [59]. The largest difference between the calculated and experimental Ru-oxo distances is 0.028 Å, which is of typical accuracy for metal-oxo distances obtained from DFT calculations [60]. The optimized structure of *cis*-$[Ru^{VI}(Me_3tacn)O_2(CF_3CO_2)]^+$ was used for subsequent TD-DFT calculation with SAOP/TZ2P. TD-DFT simulated spectrum of *cis*-$[Ru^{VI}(Me_3tacn)O_2(CF_3CO_2)]^+$ in gas phase is depicted in Fig. 6. Selected calculated electronic transitions are listed in Table A1 in the Appendix. The simulated spectrum comprises a weak band at 600 nm and a broad band at about 350–400 nm. The weak band at 600 nm is attributed to HOMO → LUMO ($Ru(d_\pi)$–$O_{oxo}(p_\pi)$ → $Ru(d_\pi)$–$O_{oxo}(p_{\pi^*})$) and HOMO → LUMO+1 ($Ru(d_\pi)$–$O_{oxo}(p_\pi)$ → $Ru(d_\pi)$–$O_{oxo}(p_{\pi^*})$) in which HOMO, LUMO, and LUMO+1 have significant Ru parentage (≈50%) (see Fig. 7). Therefore, the transition at 600 nm is *d*–*d* in nature and its λ_{max} compares well with the experimental absorption band at 695 nm having ε of ≈50 dm^3 mol^{-1} cm^{-1}. The calculated broad transition at ≈350–400 nm is composed of three transitions (λ = 389, 345, and 339 nm). The three transitions arise from HOMO-3 → LUMO ($O_{acetate}(p_\pi)$ → $Ru(d_\pi)$–$O_{oxo}(p_{\pi^*})$), HOMO-2 → LUMO+1 ($O_{oxo}(p_\pi)$–$N_{Me3tacn}(p_\pi)$ → $Ru(d_\pi)$–$O_{oxo}(p_{\pi^*})$) and HOMO-4 → LUMO+1 ($O_{acetate}(p_{\pi^*})$–$N_{Me3tacn}(p_\sigma)$ → $Ru(d_\pi)$–$O_{oxo}(p_{\pi^*})$). The simulated absorption peak at ≈350–400 nm is therefore ligand-to-metal charge transfer (LMCT) in nature, which is reminiscent of the intense broad absorption peak at 329 nm (ε = 2400 dm^3 mol^{-1} cm^{-1}) in experimental UV–vis absorption spectrum of *cis*-$[Ru^{VI}(Me_3tacn)O_2(CF_3CO_2)]^+$ in 0.1 mol dm^{-3} CF_3CO_2H [58]. Molecular orbital plots and composition of frontier orbitals are depicted in Fig. 7 and Table A2 in the Appendix.

Table 2
Selected bond distances (Å) and bond angles (°) of the singlet ground state of *cis*-$[Ru^{VI}(Me_3tacn)O_2(CF_3CO_2)]^+$.

	PBE0/SDD/6-31G*	Experimental data
Ru–N1	2.186 (0.089[a])	2.097
Ru–N2	2.286 (0.061[a])	2.225
Ru–N3	2.253 (0.057[a])	2.196
Ru–O1	1.691 (−0.028[a])	1.719
Ru–O2	1.690 (−0.022[a])	1.712
Ru–O3	1.976 (−0.069[a])	2.045
Ru–O1–C10	117.9 (−4.5[a])	122.4
O2–Ru–O3	122.2 (3.9[a])	118.3

[a] Relative error, calculated bond length minus experimental bond length.

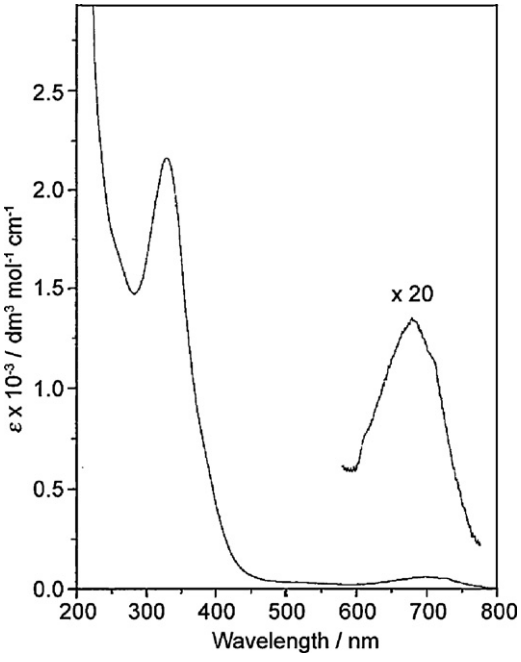

Fig. 5. UV–vis spectrum of *cis*-$[Ru^{VI}(Me_3tacn)O_2(CF_3CO_2)]ClO_4$ in 0.1 mol dm^{-3} CF_3CO_2H [58].

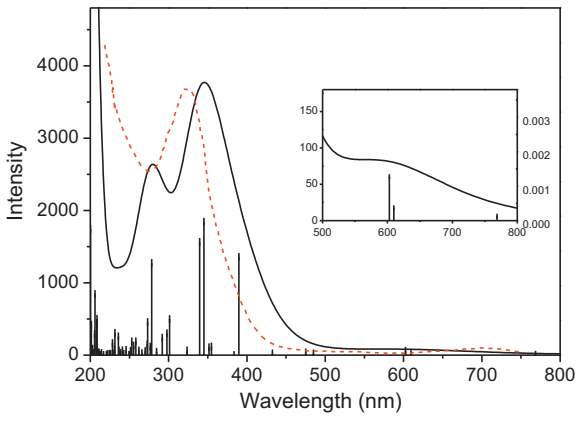

Fig. 6. Computed electronic spectrum (black solid line) of *cis*-$[Ru^{VI}(Me_3tacn)O_2(CF_3CO_2)]^+$ at the SAOP/TZ2P//PBE0/SDD/6-31G* level as compared with the experimental electronic spectrum (red dashed line) of the same complex.

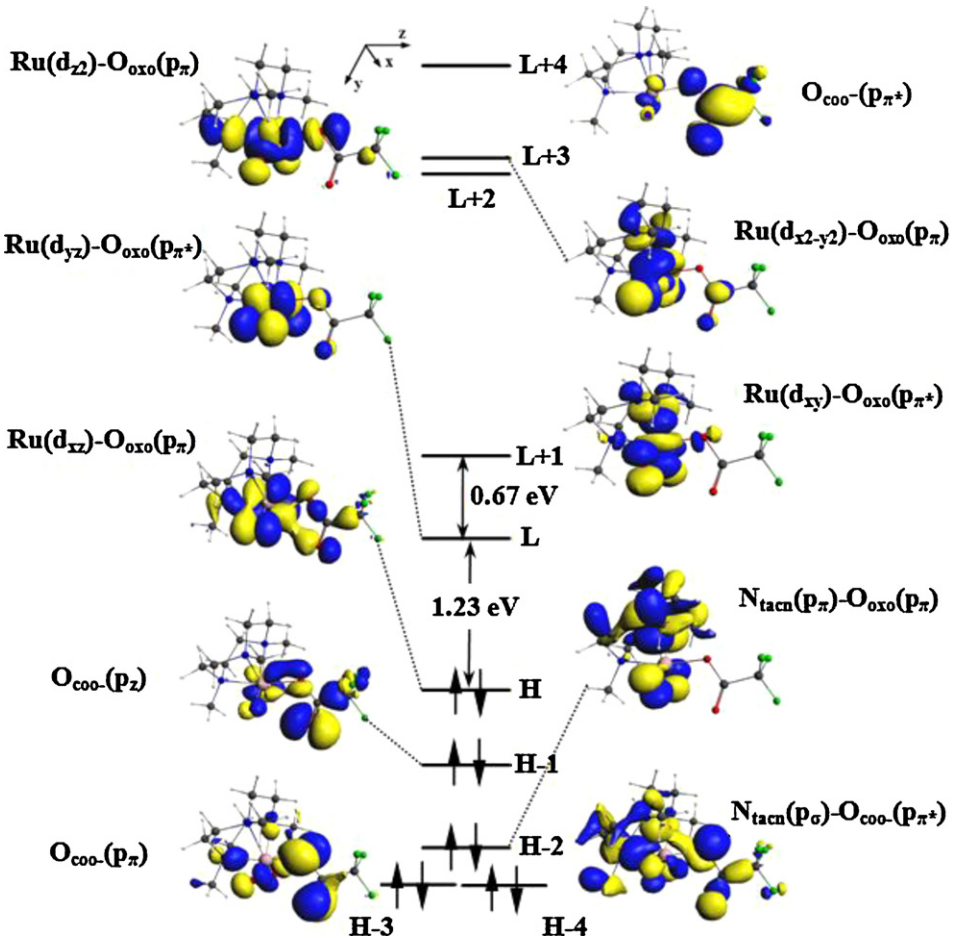

Fig. 7. Kohn-Sham MOs (isovalue = 0.03 au) and the energy scheme of *cis*-$[Ru^{VI}(Me_3tacn)O_2(CF_3CO_2)]^+$.

3.3. Concerted [3+2] cycloaddition reactions with alkynes

cis-$[Ru^{VI}(Me_3tacn)O_2(CF_3CO_2)]^+$ is a powerful oxidant; it can undergo oxidation with a variety of organic substrates including the unactivated hydrocarbon cyclohexane [17,46,47]. Among these oxidation reactions are oxygenation of unactivated saturated hydrocarbons, oxidation of dialkylsulfides to dialkylsulfoxides (Scheme 4), four-electron oxidation reaction with alkynes to α,β-diketones (Scheme 5), *cis*-dihydroxylation of alkenes to *cis*-diols, and oxidative C=C bond cleavage of alkenes to carbonyl compounds at room temperature.

Reaction of *cis*-$[Ru^{VI}(Me_3tacn)O_2(CF_3CO_2)]^+$ with diphenylacetylene gave a dark blue solution instantaneously which gradually decolorized within 30 min giving a pale yellow solution. A similar observation was also found with other disubstituted alkynes [46]. An exception to these was the reaction of *cis*-$[Ru^{VI}(Me_3tacn)O_2(CF_3CO_2)]^+$ with bis(trimethylsilyl)acetylene in which the intensely colored solution was stable over a period of 24 h. Evaporation of the solution gave crystals of $[Ru^{IV}(Me_3tacn)\{OC(SiMe_3)=C(SiMe_3)O\}(CF_3CO_2)]^+$, the X-ray crystal structure of which reveals the two *cis* oxo ligands added to the acetylenic carbon atoms forming an anionic catecholate-like ligand bonded to Ru(IV) (Fig. 8). The isolation

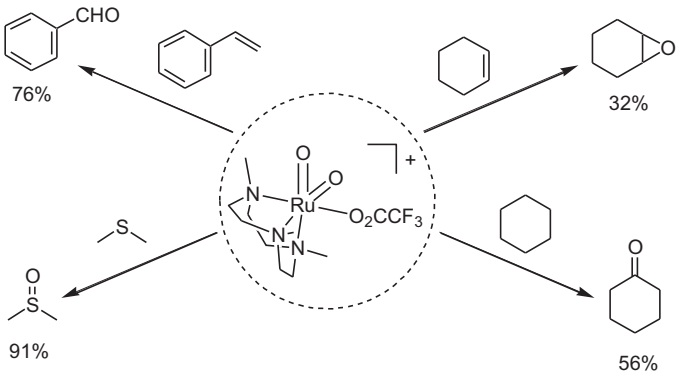

Scheme 4.

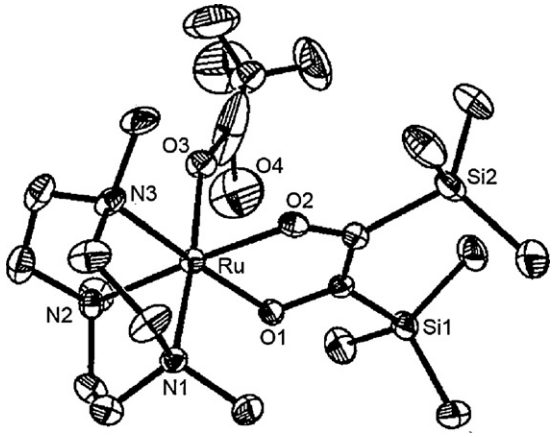

Fig. 8. Structure of $[Ru^{IV}(Me_3tacn)\{OC(SiMe_3)=C(SiMe_3)O\}(CF_3CO_2)]ClO_4$ with omission of hydrogen atoms and perchlorate ion [46].

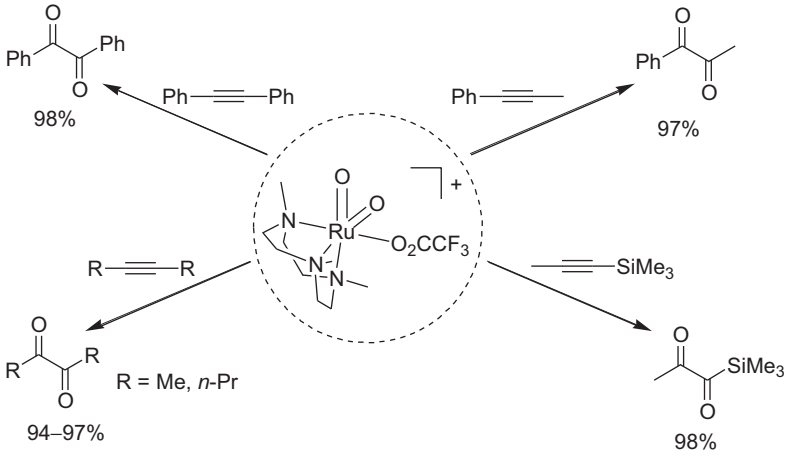

Scheme 5.

of $[Ru^{IV}(Me_3tacn)\{OC(SiMe_3)=C(SiMe_3)O\}(CF_3CO_2)]^+$, to the best of our knowledge, gives the first proof to the long proposed [3+2] cycloaddition of *cis*-dioxometal unit with C=C and C≡C bonds. Kinetic and product studies revealed that the reaction (Scheme 6) involves the formation of a vinyl radical which then collapses quickly giving the [3+2] cycloaddition product $[Ru^{IV}(Me_3tacn)\{OC(SiMe_3)=C(SiMe_3)O\}(CF_3CO_2)]^+$; this complex is further reduced to *cis*-$[Ru^{II}(Me_3tacn)(CF_3CO_2)(MeCN)_2]^+$ with the release of the diketo organic products.

3.4. Concerted [3+2] cycloaddition reactions with alkenes

[3+2] cycloaddition reactions of *cis*-$[Ru^{VI}(Me_3tacn)O_2(CF_3CO_2)]^+$ with alkenes similar to those with alkynes have been observed. However, depending on the reaction conditions, *cis*-$[Ru^{VI}(Me_3tacn)O_2(CF_3CO_2)]^+$ reacted with alkenes to give either *cis*-dihydroxylation or C=C bond cleavage products [47]. Reaction of *cis*-$[Ru^{VI}(Me_3tacn)O_2(CF_3CO_2)]^+$ with alkenes in aqueous *tert*-butyl alcohol stereoselectively afforded *cis*-dihydroxylation products (Scheme 7) in 60–85% yields, whereas oxidative cleavage of C=C bond was observed if the reaction was conducted in dry MeCN (Scheme 8).

Similar to the reaction with alkyne, the reaction of *cis*-$[Ru^{VI}(Me_3tacn)O_2(CF_3CO_2)]^+$ with alkene instantaneously generated a species with an intense absorption peak at λ_{max} = 396 nm corresponding to a Ru(III) [3+2] cycloadduct, which collapsed quickly to give the μ-oxo bridged dinuclear Ru(III) product $[\{Ru^{III}(Me_3tacn)\}_2(\mu\text{-}O)(\mu\text{-}CF_3CO_2)_2](ClO_4)_2$.

With cyclooctene and *trans*-β-methylstyrene as substrates and in aqueous *tert*-butyl alcohol, crystals of the cycloadducts $[Ru^{III}(Me_3tacn)(CF_3CO_2)\{HOCH(CH_2)_6C(H)O\}]ClO_4$ and $[Ru^{III}(Me_3tacn)(CF_3CO_2)\{HOCH(Ph)CH(Me)O\}]ClO_4$ were obtained. Crystal structure analysis of the two complexes revealed that the dioxo ligands are added to the alkenic carbons forming a glycolate chelate to the Ru(III) center (Fig. 9) [47]. In aqueous medium, $[Ru^{III}(Me_3tacn)(CF_3CO_2)\{HOCH(CH_2)_6C(H)O\}]ClO_4$ was unstable and underwent hydrolysis to form the dinuclear Ru(III) complex $[\{Ru^{III}(Me_3tacn)\}_2(\mu\text{-}O)(\mu\text{-}CF_3CO_2)_2](ClO_4)_2$ with the release of the *cis*-diol product. Neither of the oxygen atoms of the released *cis*-diol came from water, as revealed by the ^{18}O-labeling studies [47] (Scheme 9).

Kinetic and product studies suggested that the *cis*-dihydroxylation involves a concerted [3+2] cycloaddition mechanism. *cis*-$[Ru^{VI}(Me_3tacn)O_2(CF_3CO_2)]^+$ reacts with alkene to form a Ru(IV) cycloadduct which would either be reduced to

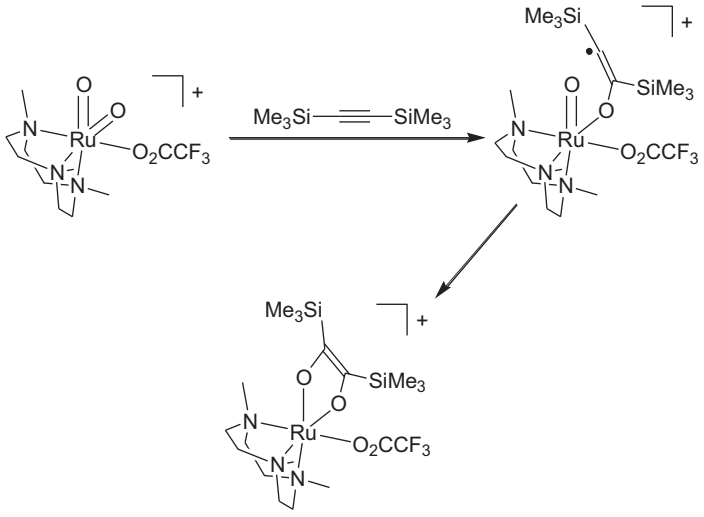

Scheme 6.

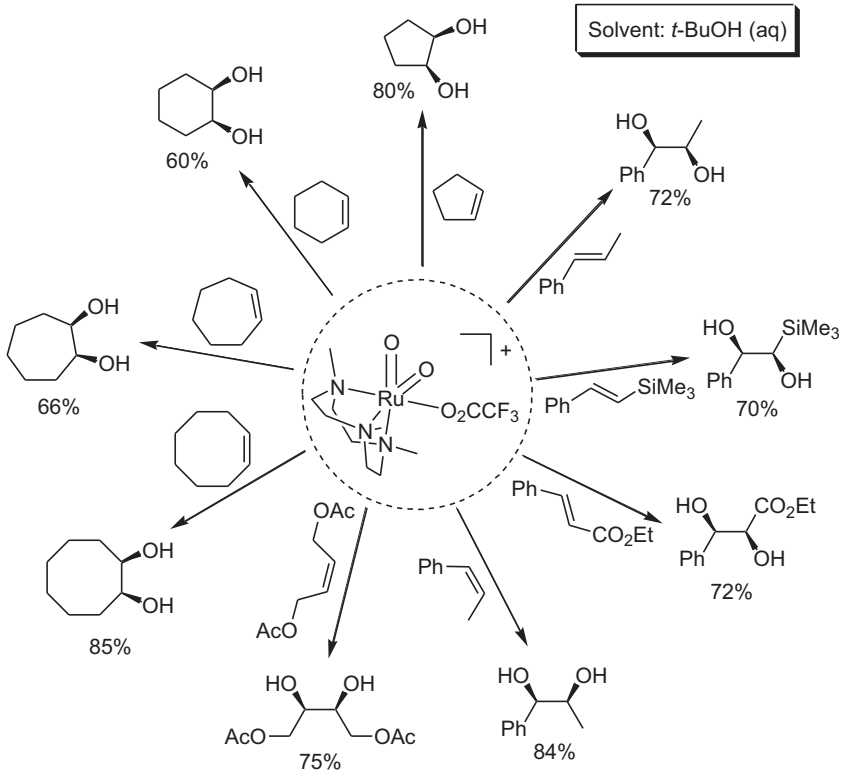

Scheme 7.

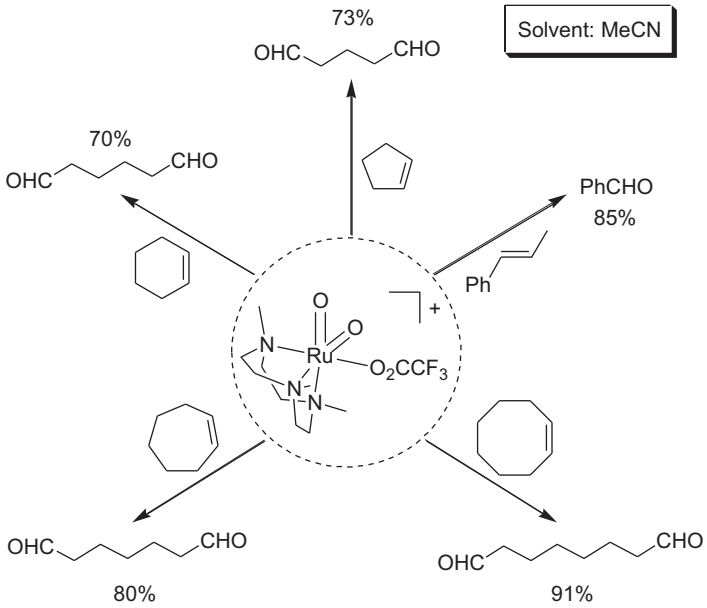

Scheme 8.

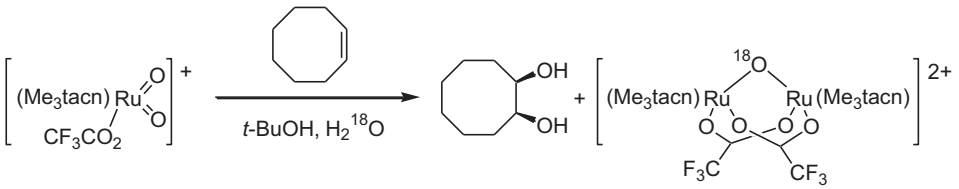

Scheme 9.

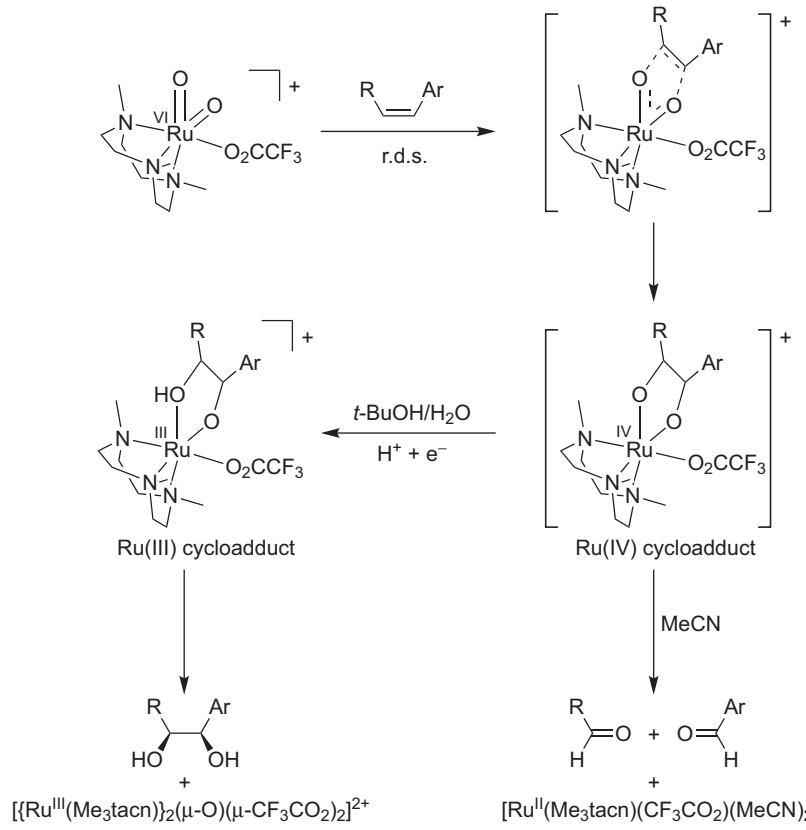

Scheme 10.

Ru(III) or undergo oxidative C–C bond cleavage to give carbonyl products depending on the reaction conditions [47] (Scheme 10).

4. Ruthenium–nitrogen multiple bonded complexes

Up to now, there have been no reports on successful isolation of Ru–Me_3tacn complexes bearing terminal nitrido and imido ligands. As discussed in latter section, these complexes are important reaction intermediates in the oxidative C–N bond formation catalyzed by Ru–Me_3tacn complexes. Ligand substitution reaction of Ru(II) in situ generated by the reduction of Ru(III) is used to prepare Ru–NH_3 and Ru–NH_2R complexes. $[Ru^{II}(Me_3tacn)(NH_3)_3](PF_6)_2$ was synthesized and obtained as a yellow solid from reduction of $[Ru^{III}(Me_3tacn)Cl_3]$ or $[Ru^{III}(Me_3tacn)(OH_2)(CF_3CO_2)_2]CF_3CO_2$ by Zn/Hg [55,61] followed by subsequent reaction with hydrazine in water. This complex has been characterized by elemental analyses, ^{1}H NMR spectroscopy, UV–vis absorption spectroscopy (λ_{max} 338 nm), and ESI-MS [61]. Its structure has been determined by X-ray crystallography (Ru–NH_3 distances 2.169(6)–2.193(9) Å) [61]. In MeCN solution, it shows a reversible Ru(III)/Ru(II) couple at $E_{1/2}$ value of 0.10 V vs. Ag/$AgNO_3$ (0.1 mol dm^{-3} in MeCN) [61].

Attempts were made to prepare Ru–Me_3tacn complexes having arylamine ligand. The reaction of $[Ru^{III}(Me_3tacn)(OH_2)(CF_3CO_2)_2]CF_3CO_2$ with aniline in the presence of Zn/Hg in water gave $[Ru^{II}(Me_3tacn)(\eta^6\text{-}PhNH_2)]^{2+}$ isolated as a yellow PF_6^- salt with its structure determined by X-ray crystallography [55]. Interestingly, aniline is π coordinated to the $[Ru^{II}(Me_3tacn)]^{2+}$ fragment via the aryl ring instead of being σ coordinated to Ru(II) via the nitrogen atom.

Coordinated RNH_2 ligand in Ru(II) complexes easily undergoes solvolysis reaction; for this reason, we designed and synthesized the following tridentate ligand bearing a 1° NH_2 group but without α C–H bond(s). The reaction of $[Ru^{III}(Me_3tacn)(OH_2)(CF_3CO_2)_2]CF_3CO_2$ with α-(1-amino-1-methylethyl)-2-pyridinemethanol (H_3L) in the presence of Zn/Hg in water under reflux conditions for 24 h gave $[Ru(Me_3tacn)(H_2L)]^{2+}$ isolated as a ClO_4^- salt with its structure determined by X-ray crystallography (Fig. 10). The OH group of the H_3L ligand is deprotonated and the Ru–O distance of 1.941(2) Å is comparable to related Ru–O distances of 1.902(3) and 1.921(3) Å in [Ru(L′)NCl] (L′ = 2,6-bis(2,2-diphenyl-2-hydroxyethyl)pyridine) [55]. Using Evans method, $[Ru(Me_3tacn)(H_2L)]^{2+}$ is paramagnetic with μ_{eff} of 1.74 μ_B characteristic of Ru(III) formulation.

We have made attempts to generate reactive ruthenium-imido complexes of Me_3tacn by chemical and electrochemical oxidation reactions. Oxidation of $[Ru^{II}(Me_3tacn)(NH_3)_3]^{2+}$ with $[NH_4]_2[Ce(NO_3)_6]$ in water gave $[Ru^{II}(Me_3tacn)(NH_3)_2(NO)]^{3+}$ isolated as a PF_6^- salt [61]. With reference to previous works by Meyer and co-workers [62], it is likely that an oxidizing Ru≡N reaction intermediate in oxidation state of Ru(V) or Ru(VI) was generated in situ, which underwent reaction with H_2O or OH^- to give Ru–NO species.

In aqueous solution, $[Ru(Me_3tacn)(H_2L)]^{2+}$ undergoes intriguing electrochemical oxidation reactions. Its cyclic voltammogram in 0.1 mol dm^{-3} CF_3CO_2H shows a reversible couple with $E_{1/2}$ = 0.21 V vs. SCE and an irreversible oxidative wave with E_{pc} = 1.53 V vs. SCE [55]. The $E_{1/2}$ and E_{pc} values of the reversible couple and irreversible oxidation wave are pH dependent, both of which shift negatively with a slope of −60 mV/pH at pH ranging from 1.0 to 7.0.

Rotating disc voltammetry experiments conducted in aqueous buffer solution at pH 6–7 revealed that the plateau currents for the reversible couple and the irreversible oxidative wave are in a ratio of 1:2. As the plateau current of the reversible couple has a similar value as that for the $[Fe(CN)_6]^{3-/4-}$ couple under same experimental conditions, the electrochemical oxidation reactions depicted in Scheme 11 are assigned.

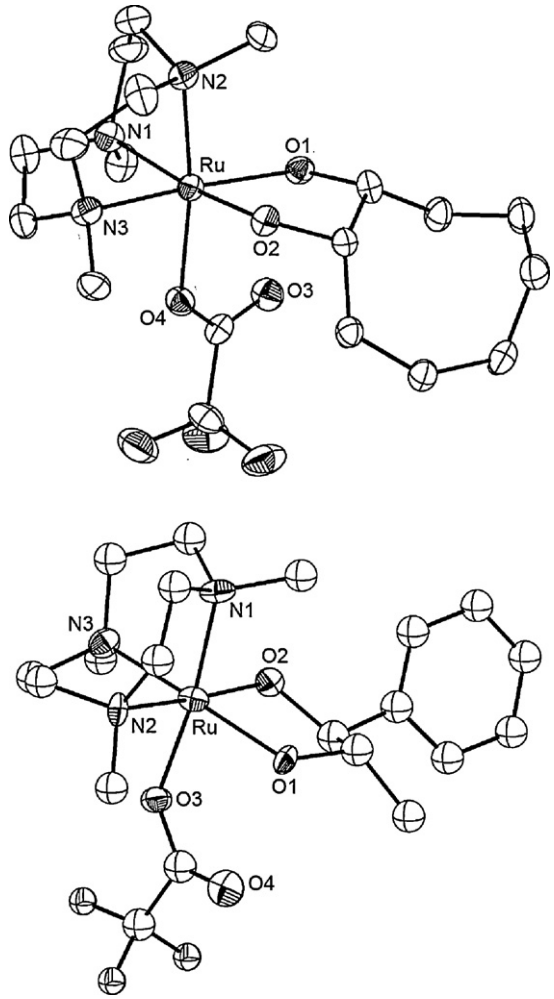

Fig. 9. Structures of $[Ru^{III}(Me_3tacn)(CF_3CO_2)\{HOCH(CH_2)_6C(H)O\}]ClO_4$ (top) and $[Ru^{III}(Me_3tacn)(CF_3CO_2)\{HOCH(Ph)CH(Me)O\}]ClO_4$ (bottom) with omission of hydrogen atoms and perchlorate ions [47].

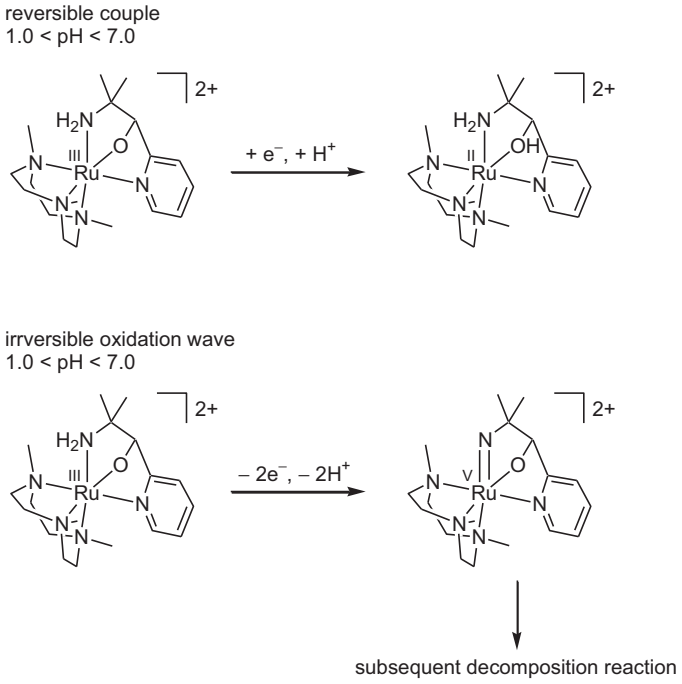

Scheme 11.

Because of the chelation nature of the deprotonated ligand L, the electrochemically generated Ru(V)-imido complex of L would adopt a bent Ru–N–C instead of a linear Ru–N–C geometry expected for a complex having a terminal alkylimido ligand, thus accounting for the instability of the electrochemically generated $[Ru^V(Me_3tacn)(L)]^{2+}$ and the irreversible nature of the electrochemical oxidation.

In our attempts to prepare Ru–Me_3tacn complexes containing tosylamido and tosylimido ligands, we treated $[(Me_3tacn)Ru^{III}Cl_3]$ with TsNHNa in methanol at room temperature for 3 h, and obtained $[Ru^{III}(Me_3tacn)(NHTs)_2(OH)]$ as a yellow crystalline solid; its formulation is supported by X-ray crystal structure determination (Fig. 11) and magnetic susceptibility measurement ($\mu_{eff} = 1.8\ \mu_B$) [54a].

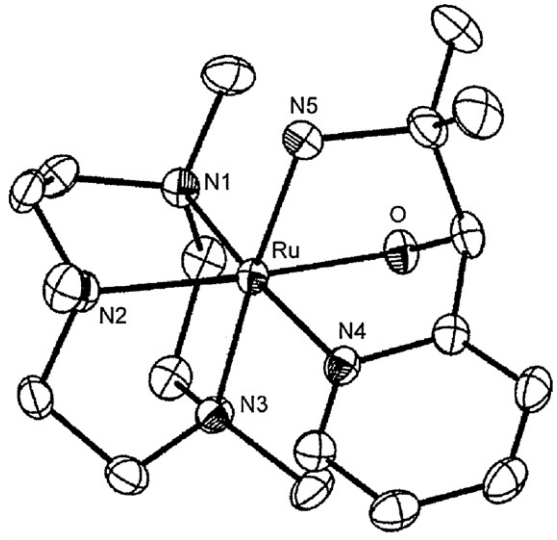

Fig. 10. Structure of $[Ru^{III}(Me_3tacn)(H_2L)](ClO_4)_2$ with omission of hydrogen atoms and perchlorate ion [55].

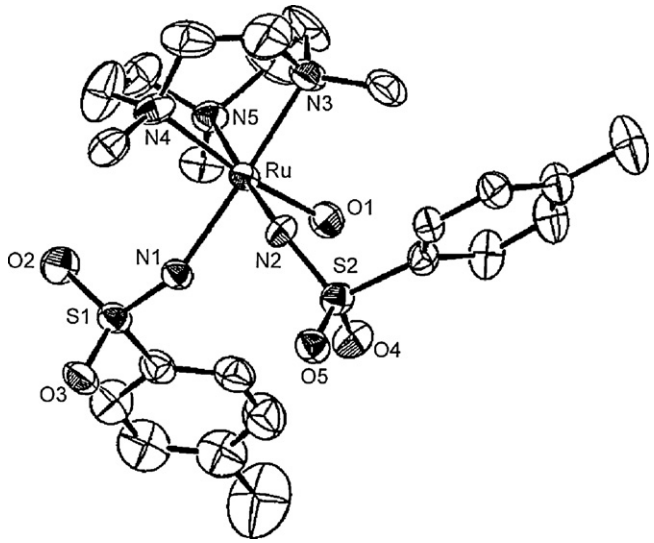

Fig. 11. Structure of $[Ru^{III}(Me_3tacn)(NHTs)_2(OH)]$ with omission of hydrogen atoms [54a].

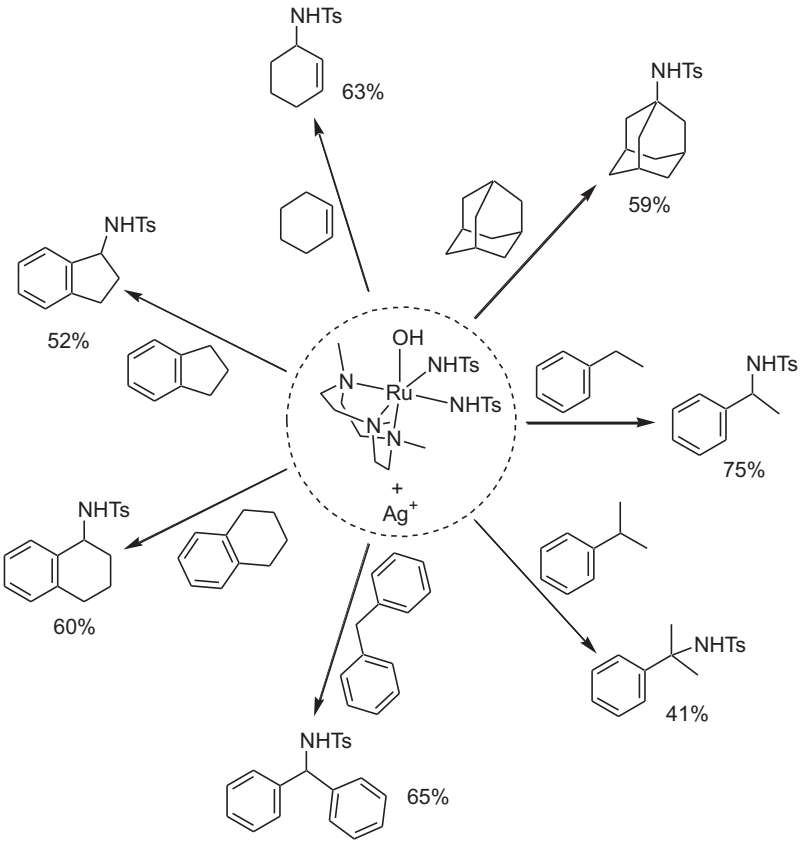

Scheme 12.

Upon oxidation of $[Ru^{III}(Me_3tacn)(NHTs)_2(OH)]$ with $AgClO_4$ in MeCN, a red species with λ_{max} = 480 nm was obtained (Fig. 12) [54a,63]. This red species could stoichiometrically react with various saturated C–H bonds including an adamantane 3° C–H bond and allylic and benzylic C–H bonds to afford the corresponding *N*-tosylamines in 41–75% yields [54a] (Scheme 12). These amination reactions became catalytic by using PhI=NTs as nitrogen source and $[Ru^{III}(Me_3tacn)(NHTs)_2(OH)]$ as catalyst (see later section). Thus the question is: *what is the nature of the red species with λ_{max} = 480 nm generated upon oxidation of $[Ru^{III}(Me_3tacn)(NHTs)_2(OH)]$ with $AgClO_4$?* We conceive that this red species is a reactive Ru=NTs species bearing a Me_3tacn ligand. This speculation is supported by experiment and our recent TD-DFT calculations (see Appendix for computational details). Experimentally, the transformation of (1-cyclohexenyloxy)trimethylsilane to α-*N*-tosylaminocyclohexanone by the "$[Ru^{III}(Me_3tacn)(NHTs)_2(OH)] + AgClO_4$" protocol is similar to that reported by the "[(Schiff base)Mn^{V}≡N] + $(CF_3CO)_2O$" [64] and "Cu(I) + PhI=NTs" [65] systems; the latter two systems are widely conceived to involve a reactive metal-tosylimido/nitrene reaction intermediate. The effect of *para*-substituents on the amination of substituted ethylbenzenes by the red species has been examined by competitive experiments [54a]. A linear free energy relationship has been obtained with negative ρ^+ value of −0.67 revealing the electrophilic nature of the red species [54a].

To investigate this red species, the hypothetical $[Ru(Me_3tacn)(NBs)(NHBs)(MeCN)]^+$ and $[Ru(Me_3tacn)(NBs)_2(OH)]^+$ (Bs = benzenesulfonyl) complexes (Fig. 13) were computed with both of their structures optimized with PBE0/SDD/6-31G*. These model complexes were constructed using the bis-tosylamido complex $[Ru(Me_3tacn)(NHTs)_2(OH)]$ as a

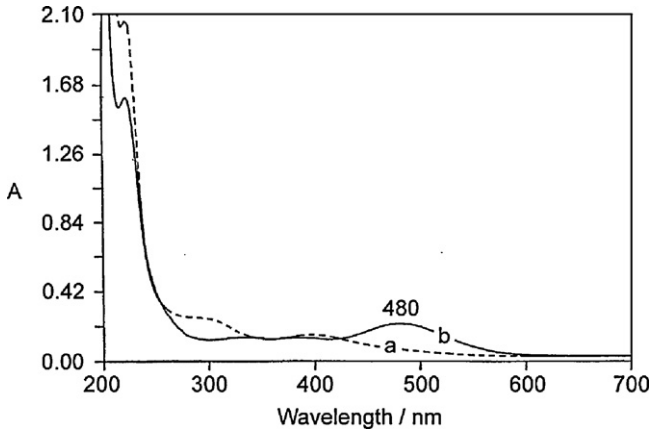

Fig. 12. UV–vis spectra of $[Ru^{III}(Me_3tacn)(NHTs)_2(OH)]$ in MeCN before (a) and after (b) addition of $AgClO_4$ [63].

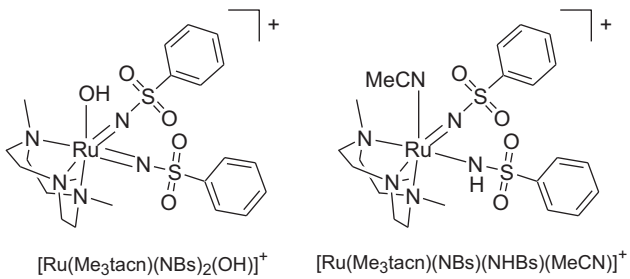

Fig. 13. Structures of model bis- and mono-arenesulfonylimido ruthenium complexes.

starting reference for a DFT energy minimization. The PBE0/SDD/6-31G* results could reproduce the experimental X-ray crystal structure of $[Ru(Me_3tacn)(NHTs)_2(OH)]$ [54a], in which the calculated N–S distances are longer by as much as 0.066 Å compared with the experimental values. For $[Ru(Me_3tacn)(NBs)_2(OH)]^+$, PBE0/SDD/6-31G* energy minimized structure in singlet ($S=0$) is 5.0 kcal mol^{-1} lower in energy than in triplet ($S=1$). However, for $[Ru(Me_3tacn)(NBs)(NHBs)(MeCN)]^+$, the PBE0 predicted a triplet ground state (6.75 kcal mol^{-1} more favored than singlet). Here, we discuss the electronic structures and spectroscopic properties with PBE0/SDD/6-31G* optimized singlet structures. TD-DFT simulated UV–vis absorption spectra of $[Ru(Me_3tacn)(NBs)(NHBs)(MeCN)]^+$ and $[Ru(Me_3tacn)(NBs)_2(OH)]^+$ with SAOP/TZ2P are shown in Fig. 14. *Incidentally, both spectra show an absorption peak at ≈450–500 nm, similar to the 480 nm of the red species.* For $[Ru(Me_3tacn)(NBs)(NHBs)(MeCN)]^+$, the absorption peak at ≈450 nm is attributed to transition from HOMO-6 → LUMO ($Ph(p_\pi) \rightarrow Ru(d_\pi)$–$N_{NBs}(p_{\pi^*})$, Ru parentage ≈50%) whereas for $[Ru(Me_3tacn)(NBs)_2(OH)]^+$ the absorption peak at ≈500 nm is ascribed to transitions from HOMO-4 → LUMO+1 ($N_{NBs}(p_\pi) \rightarrow Ru(d_\pi)$–$N_{NBs}(p_{\pi^*})$, Ru parentage ≈40%) and HOMO-5 → LUMO+1 ($Ph(p_\pi) \rightarrow Ru(d_\pi)$–$N_{NBs}(p_{\pi^*})$).

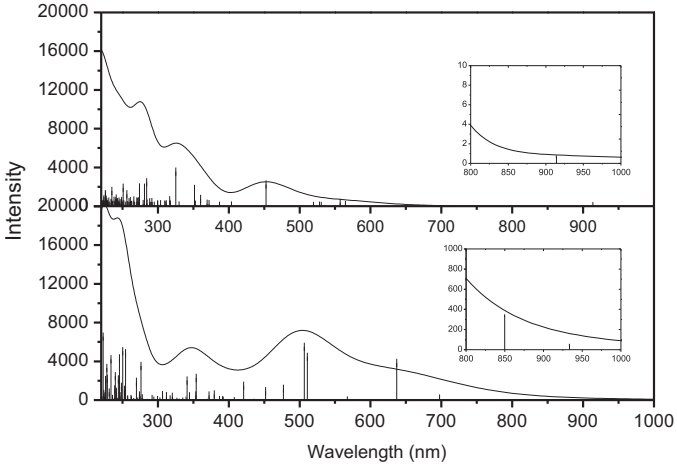

Fig. 14. Simulated absorption spectra of $[Ru(Me_3tacn)(NBs)(NHBs)(MeCN)]^+$ (top) and $[Ru(Me_3tacn)(NBs)_2(OH)]^+$ (bottom) with TD-SAOP/TZ2P//PBE0/SDD/6-31G* in gas phase.

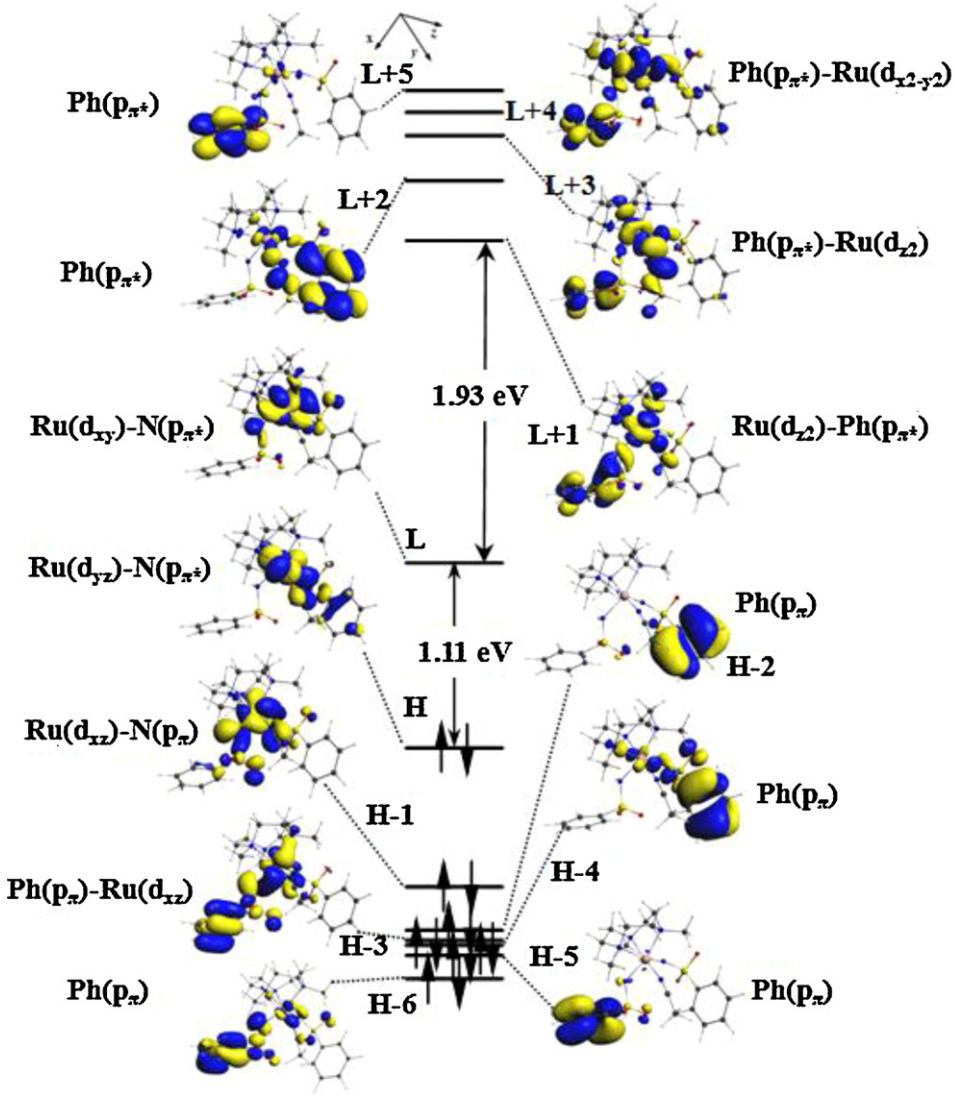

Fig. 15. Kohn-Sham MOs (isovalue = 0.03 au) and the energy scheme of $[Ru(Me_3tacn)(NBs)(NHBs)(MeCN)]^+$.

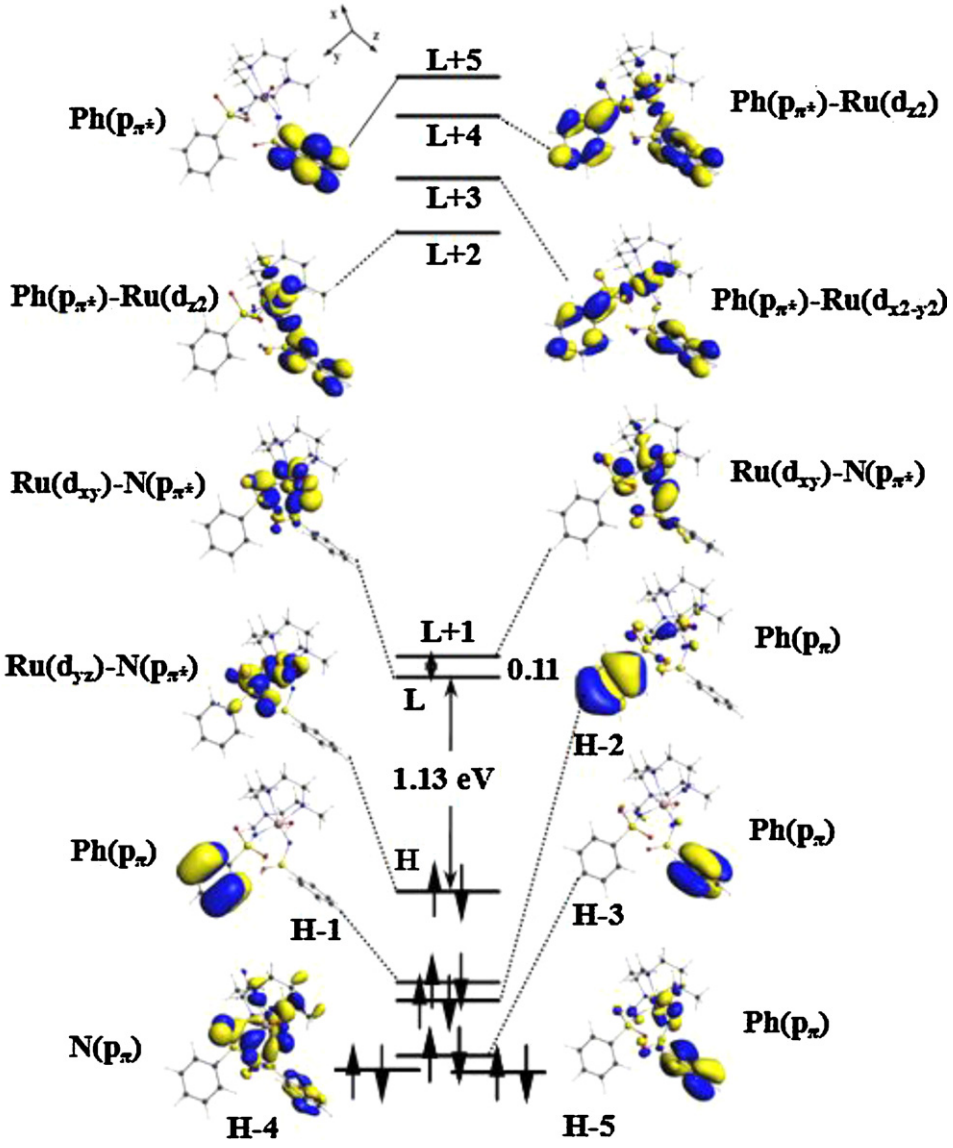

Fig. 16. Kohn-Sham MOs (isovalue = 0.03 au) and the energy scheme of $[Ru(Me_3tacn)(NBs)_2(OH)]^+$.

Selected list of calculated vertical excitations, frontier orbital energies and contributions, and surface plot of frontier molecular orbitals for $[Ru(Me_3tacn)(NBs)(NHBs)(MeCN)]^+$ and $[Ru(Me_3tacn)(NBs)_2(OH)]^+$ can be found in Tables A3–6 in the Appendix and Figs. 15 and 16.

Importantly the 480 nm absorption of the red species has a close resemblance to the TD-DFT calculated UV–vis absorption spectrum of $[Ru(Me_3tacn)(NBs)_2(OH)]^+$ in the 400–550 nm region, and that of $[Ru(Me_3tacn)(NBs)(NHBs)(MeCN)]^+$ also shows a strong absorption band in this region, though less resolved. The computational results are therefore supportive of the red species [obtained by oxidation of $[Ru(Me_3tacn)(NHTs)_2(OH)]$ with Ag(I)] to be a reactive Ru=NTs complex.

5. Ruthenium-catalyzed oxidation and amination reactions

In contrast to the use of dinuclear catalysts in oxidation reactions catalyzed by Me_3tacn complexes of manganese [10] and iron [13], mononuclear ruthenium Me_3tacn complexes have been reported as efficient catalysts for oxidative catalysis [17,45,48–54]; these ruthenium-catalyzed reactions, developed by our group, are summarized in this section. For ruthenium complexes of other tacn derivatives, Süss-Fink and co-workers reported oxidation of isopropanol with H_2O_2 in water catalyzed by dinuclear ruthenium Me_2tacn complex $[\{Ru^{III}(Me_2tacn)\}_2(\mu\text{-}O)(\mu\text{-}OAc)_2]^{2+}$ (Me_2tacn = 1,4-dimethyl-1,4,7-triazacyclononane) [66].

cis-$[Ru^{VI}(Me_3tacn)O_2(CF_3CO_2)]^+$ has been demonstrated to be a reaction intermediate in the $[Ru^{III}(Me_3tacn)(OH_2)(CF_3CO_2)_2]^+$-catalyzed oxidation of anisole by *t*-BuOOH [52]. As *cis*-$[Ru^{VI}(Me_3tacn)O_2(CF_3CO_2)]^+$ is highly reactive and not convenient to handle, its precursor $[Ru^{III}(Me_3tacn)(OH_2)(CF_3CO_2)_2]CF_3CO_2$, the structure of which has been determined by X-ray crystal analysis (Fig. 17, Ru–OH_2 distance: 2.111(2) Å) [49], has always been used for oxidative catalysis that proceeds through reactive Ru=O intermediate(s) of Me_3tacn.

5.1. Epoxidation of alkenes

In 1994, we reported that *cis*-$[Ru^{VI}(Me_3tacn)O_2(CF_3CO_2)]^+$ not only effected stoichiometric oxidation of hydrocarbons and dimethyl sulfide, but also catalyzed alkene epoxidation with *t*-

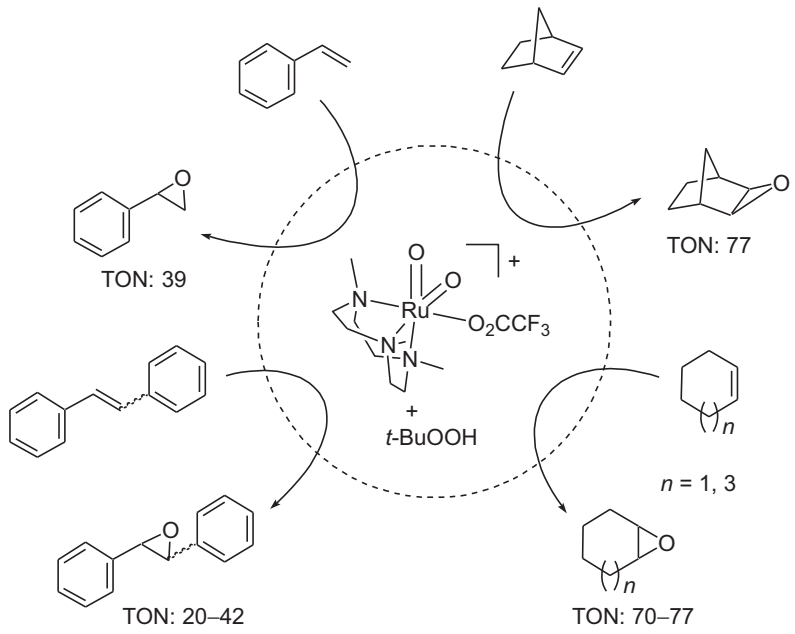

Scheme 13.

BuOOH as terminal oxidant, giving product turnovers (TON) of up to 77 [17] (Scheme 13).

Subsequently we observed efficient epoxidation of alkenes with *t*-BuOOH catalyzed by $[Ru^{III}(Me_3tacn)(OH_2)(CF_3CO_2)_2]^+$ under mild conditions [48, wherein the catalyst was incorrectly formulated as "$[Ru^{III}(Me_3tacn)(OH_2)_2(CF_3CO_2)]^{2+\prime}$], which converted styrene to styrene oxide in 78% yield. Using the "$[Ru^{III}(Me_3tacn)(OH_2)(CF_3CO_2)_2]^+$ + *t*-BuOOH" protocol, both *trans* and *cis* isomers of stilbene and β-methylstyrene can be oxidized, giving epoxides in 54–70% yields; the epoxidation of cyclohexene and cyclooctene afforded their epoxides in 85–90% yields.

Remarkable selectivity was found in subsequent epoxidation of alkenes with *t*-BuOOH catalyzed by silica gel-supported $[Ru^{III}(Me_3tacn)(OH_2)(CF_3CO_2)_2]^+$ [49]. This catalyst resulted in the conversion of norbornene and cyclooctene to their *exo* epoxides exclusively in >95% yields. While the $[Ru^{III}(Me_3tacn)(OH_2)(CF_3CO_2)_2]^+$-catalyzed oxidation of (+)-limonene with *t*-BuOOH afforded a mixture of 1,2-epoxide (54% yield) and terminal 8,9-epoxide (16% yield) [48], the same reaction catalyzed by silica gel-supported $[Ru^{III}(Me_3tacn)(OH_2)(CF_3CO_2)_2]^+$ (Scheme 14) gave 1,2-epoxide as the only isolable product (53% yield).

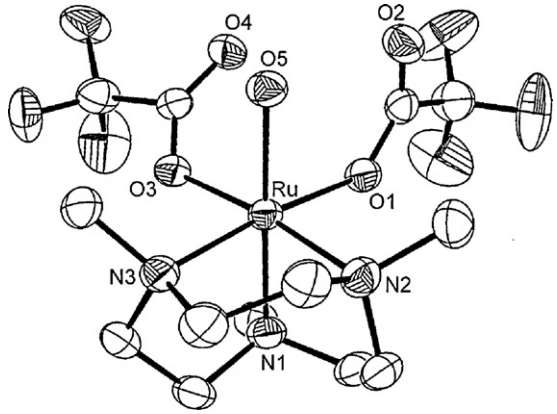

Fig. 17. Structure of $[Ru^{III}(Me_3tacn)(OH_2)(CF_3CO_2)_2]CF_3CO_2$ with omission of hydrogen atoms and counteranion [49].

5.2. Oxidation of alkanes

Using PhI=O or *t*-BuOOH as terminal oxidant, *cis*-$[Ru^{VI}(Me_3tacn)O_2(CF_3CO_2)]^+$ catalyzed the oxidation of cyclohexane, resulting in the formation of cyclohexanone with 21 and 55 turnovers, respectively [17] (Scheme 15). Cyclohexanol was formed as a minor product (18 turnovers) in the oxidation by *t*-BuOOH. $[Ru^{III}(Me_3tacn)(OH_2)(CF_3CO_2)_2]^+$ is also an active catalyst for the oxidation of cyclohexane with *t*-BuOOH, which gave cyclohexanone and cyclohexanol with total product turnovers of up to 78 [48].

5.3. Oxidation of alcohols

Not only active for alkene epoxidation and alkane oxidation, $[Ru^{III}(Me_3tacn)(OH_2)(CF_3CO_2)_2]^+$ is also an efficient catalyst for oxidation of alcohols with *t*-BuOOH [50]. A variety of primary alcohols were oxidized to aldehydes with high selectivity in 83–90% yields (Scheme 16, substrate conversions: 67–97%). The oxidation of geraniol afforded a geranial selectively, with the isolated trisubstituted C=C bonds in this substrate remaining unoxidized. By

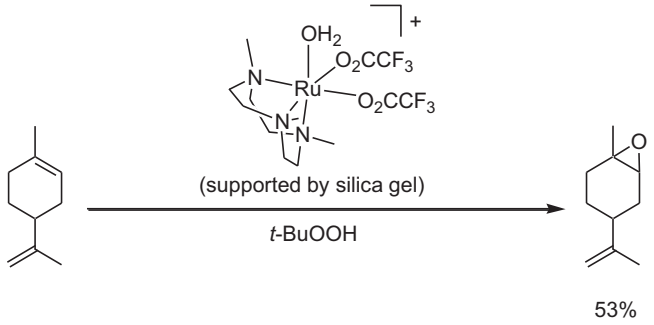

Scheme 14.

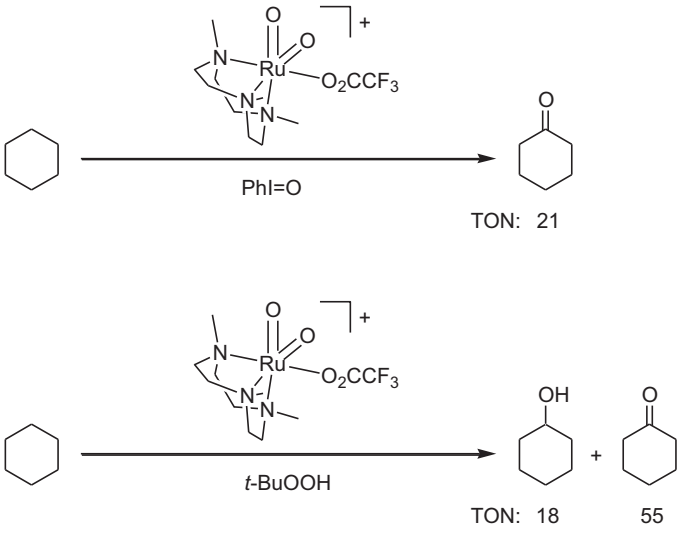

Scheme 15.

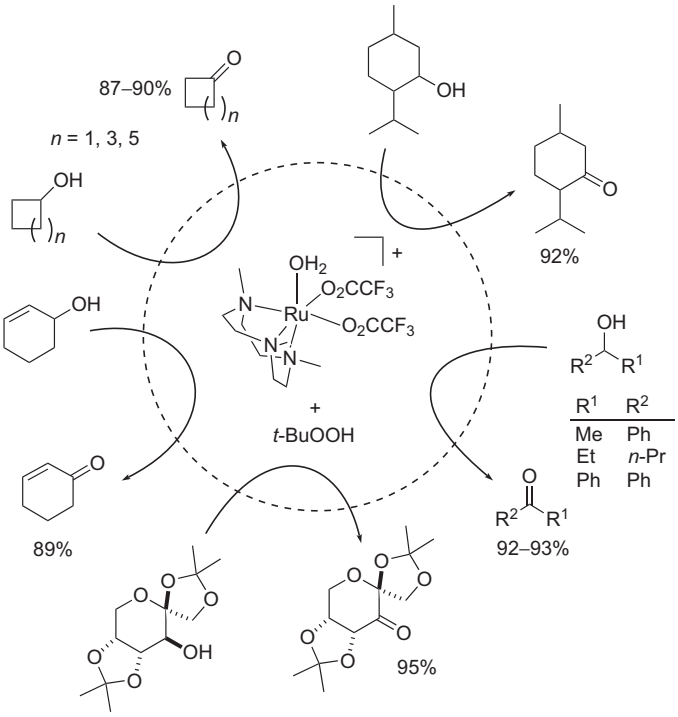

Scheme 17.

scaling up the oxidation of benzyl alcohol to a 200 mmol scale, benzaldehyde was obtained in 97% yield with 700 turnovers. Various secondary alcohols were also oxidized with high selectivity, affording ketones in 87–95% yields (Scheme 17, substrate conversions: 47–100%).

With silica gel-supported $[Ru^{III}(Me_3tacn)(OH_2)(CF_3CO_2)_2]CF_3CO_2$ as catalyst, oxidation of primary and secondary benzyl, allylic, and propargylic alcohols with *t*-BuOOH gave aldehydes and ketones in excellent yields [49]. For the allylic and propargylic alcohols, no oxidation of their C=C and C≡C bonds was observed. In the case of oxidation of 1-phenyl-1-propanol to 1-phenyl-1-propanone, the catalyst was consecutively reused eight times without significant loss of catalytic activity and selectivity; two successive reactions at a lower catalyst loading gave total turnovers of 9495.

Upon changing the terminal oxidant to aqueous H_2O_2, the oxidation of primary alcohols catalyzed by $[Ru^{III}(Me_3tacn)(OH_2)(CF_3CO_2)_2]^+$ led to the formation of carboxylic acids in 83–96% yields [51] (Scheme 18, substrate conversion: 100%). 1-Phenyl-1-ethanol, a secondary alcohol, was converted to 1-phenyl-2-ethanone in 98% yield (98 turnovers). The $[\{Ru^{III}(Me_2tacn)\}_2(\mu\text{-}O)(\mu\text{-}OAc)_2]^{2+}$-catalyzed oxidation of isopropanol with H_2O_2 in water, reported by Süss-Fink and coworkers, gave acetone with 72 turnovers [66]. We performed a one-mole scale oxidation of 1-octanol with H_2O_2 (aq) catalyzed by $[Ru^{III}(Me_3tacn)(OH_2)(CF_3CO_2)_2]^+$, which produced 129 g of 1-octanoic acid (90% yield) (Scheme 18).

5.4. Oxidation of aldehydes

In view of $[Ru^{III}(Me_3tacn)(OH_2)(CF_3CO_2)_2]^+$-catalyzed oxidation of primary alcohols with *t*-BuOOH to give aldehydes (Scheme 16), the conversion of primary alcohols to carboxylic

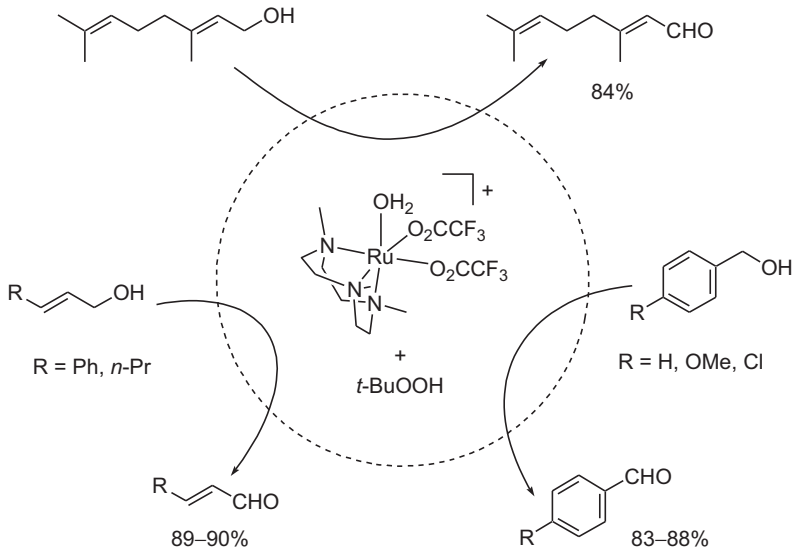

Scheme 16.

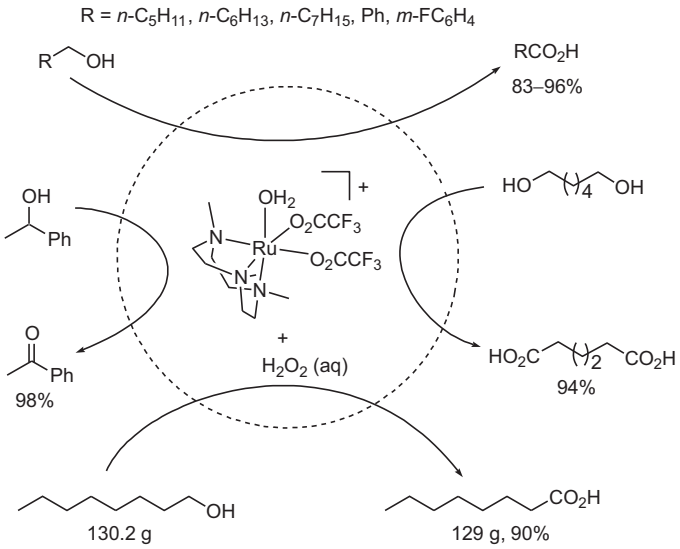

Scheme 18.

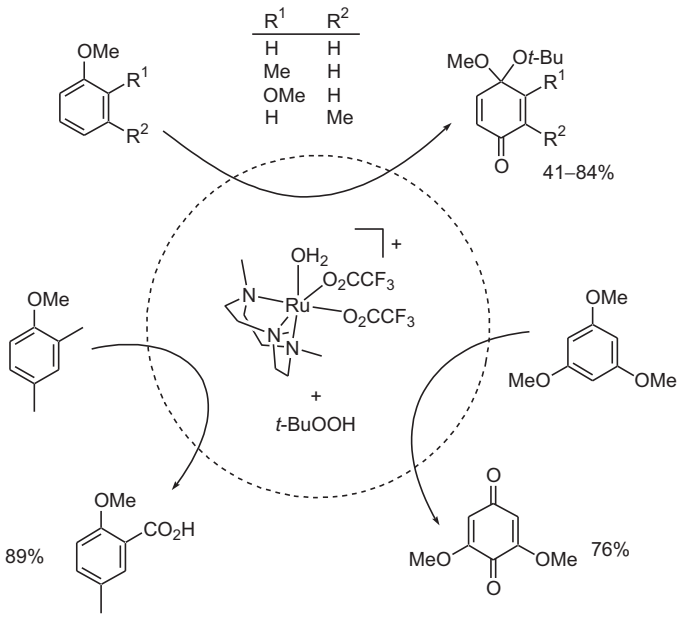

Scheme 20.

acids from oxidation with H_2O_2 (aq) catalyzed by the same complex (Scheme 18) possibly proceeded via pre-formation of aldehydes. Indeed, reaction of benzaldehyde with H_2O_2 (aq) in the presence of catalyst $[Ru^{III}(Me_3tacn)(OH_2)(CF_3CO_2)_2]^+$ afforded benzoic acid in 94% yield, and aliphatic aldehydes 1-hexanal and 1-heptanal were oxidized to the corresponding carboxylic acids in 85% and 87% yields, respectively [51] (Scheme 19, substrate conversion: 100%).

5.5. Oxidation of arenes

A series of anisoles were oxidized to *p*-benzoquinone monoketals by *t*-BuOOH in the presence of catalyst $[Ru^{III}(Me_3tacn)(OH_2)(CF_3CO_2)_2]CF_3CO_2$ [52] (Scheme 20), a reaction that can be considered as regioselective aromatic C–H oxidation. The oxidation of 2-methoxyanisole gave 3,4-dimethoxy-4-*tert*-butoxy-2,5-cyclohexadienone in 84% yield (based on the consumed substrate) and with 82% substrate conversion. For 2,4-dimethyl and 3,5-dimethoxy anisoles, the oxidation products were carboxylic acid and quinone compounds, respectively, which were formed in 89% and 76% yields (substrate conversion: 45–100%) [52].

5.6. Oxidative cleavage of C=C, C≡C, and C–C bonds

Catalyst $[Ru^{III}(Me_3tacn)(OH_2)(CF_3CO_2)_2]^+$ coupled with terminal oxidant H_2O_2 (aq) constitutes an appealing protocol for oxidation of alkenes, alkynes, and *cis*-diols, resulting in the cleavage of C=C, C≡C, and C–C bonds, respectively [51]. A series of cycloalkenes were converted to dicarboxylic acids in 85–95% yields, and the oxidation of styrenes, linear alkenes, *trans*-β-methylstyrene, and *cis*-stilbene afforded monocarboxylic acids in 78–93% yields (Scheme 21, substrate conversion: 100%). Similar product yields of 75–89% were obtained in the conversion of various mono- and disubstituted alkynes to monocarboxylic acids (Scheme 22, substrate conversion: 23–100%). For the oxidation of several *cis*-diols, carboxylic acid products were obtained in 93–97% yields (Scheme 22, substrate conversion: 100%).

One-mole scale oxidations of cyclohexene and cyclooctene by the "$[Ru^{III}(Me_3tacn)(OH_2)(CF_3CO_2)_2]^+ + H_2O_2$ (aq)" protocol have been performed [51]. These reactions afforded 124 g of adipic acid

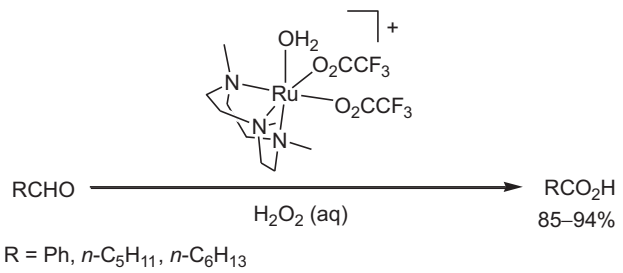

Scheme 19.

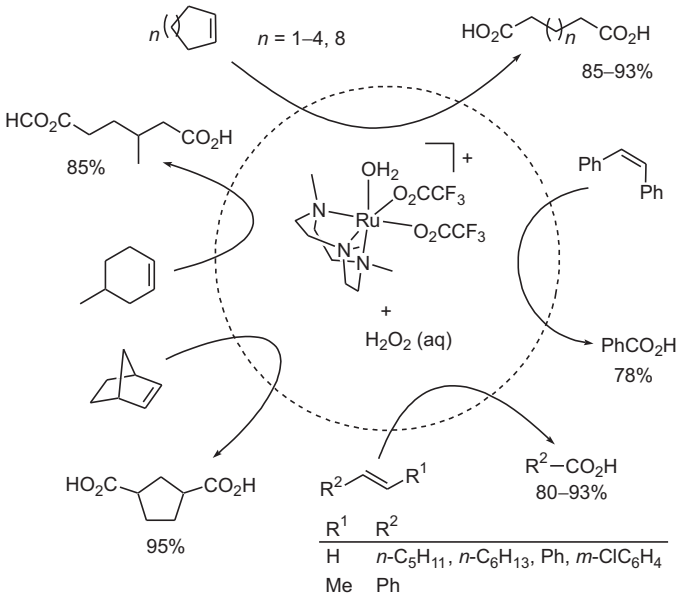

Scheme 21.

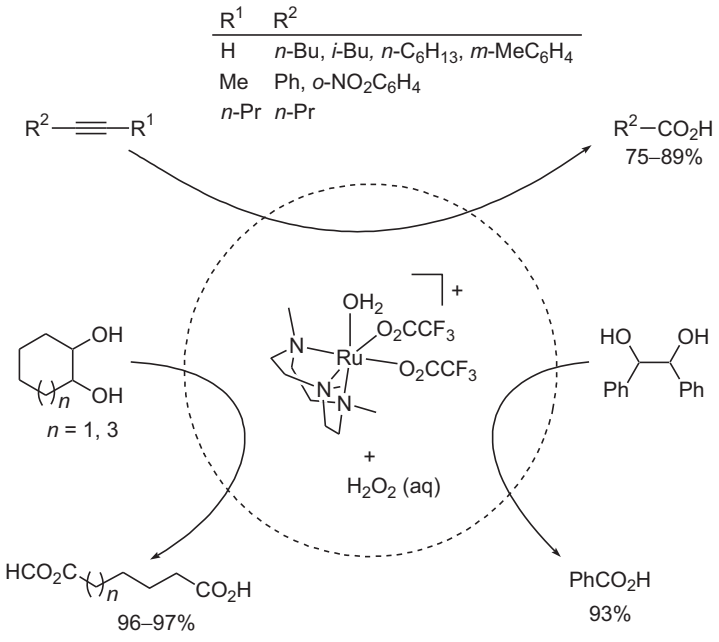

Scheme 22.

(85% yield) and 158 g of suberic acid (91% yield), respectively (Scheme 23).

5.7. *cis*-Dihydroxylation of alkenes

Recently, we reported that $[Ru^{III}(Me_3tacn)Cl_3]$ can catalyze *cis*-dihydroxylation of alkenes with H_2O_2 (aq) in the presence of additives Al_2O_3 and NaCl [53]. A variety of unfunctionalized alkenes, including cycloalkenes, aliphatic alkenes, and styrenes were selectively oxidized to *cis*-diols with up to 100% substrate conversion and in 59–96% yields (Scheme 24, substrate conversion: 60–100%). Competitive catalytic *cis*-dihydroxylation of *para*-substituted styrenes gave linear Hammett correlation with $\rho = -0.97$ ($R = 0.988$), and the cycloadduct $[Ru(Me_3tacn)\{HOCH(CH_2)_6C(H)O\}Cl]^+$ was detected by ESI-MS for the catalytic *cis*-dihydroxylation of cyclooctene. These results are similar to those of concerted [3+2] cycloaddition of *cis*-$[Ru^{VI}(Me_3tacn)O_2(CF_3CO_2)]^+$ with the same alkenes [47].

When the $[Ru^{III}(Me_3tacn)Cl_3]$-catalyzed *cis*-dihydroxylation of cycloheptene and cyclooctene were scaled up to one-mole scale, 119 g of *cis*-1,2-cycloheptanediol (91% yield) and 128 g of *cis*-1,2-cyclooctanediol (92% yield) were obtained [53] (Scheme 25). Interestingly, even in the absence of additives Al_2O_3 and NaCl, the oxidation of cycloheptene (1 mol) gave *cis*-1,2-cycloheptanediol in 89% yield (115.7 g).

5.8. Amination of saturated C–H bonds

Tremendous efforts have been devoted to develop metal Me_3tacn complexes as catalysts for organic oxidation including *cis*-dihydroxylation and epoxidation of alkenes and oxidation of other unsaturated hydrocarbons, but related studies on catalytic C–N bond formation are sparse. We have examined the feasibility of performing amination and aziridination of organic substrates catalyzed by Ru–Me_3tacn complexes. We found that catalytic amination of saturated C–H bonds can be achieved in up to 72% yield by using $[Ru^{III}(Me_3tacn)(NHTs)_2(OH)]$ as catalyst and PhI=NT as nitrogen source [54a] (Scheme 26). Up to 93% yield of the amination products was obtained upon changing the catalyst to $[Ru^{III}(Me_3tacn)(OH_2)(CF_3CO_2)_2]CF_3CO_2$ [54b] (see values in parentheses in Scheme 26, substrate conversion: 38–79%).

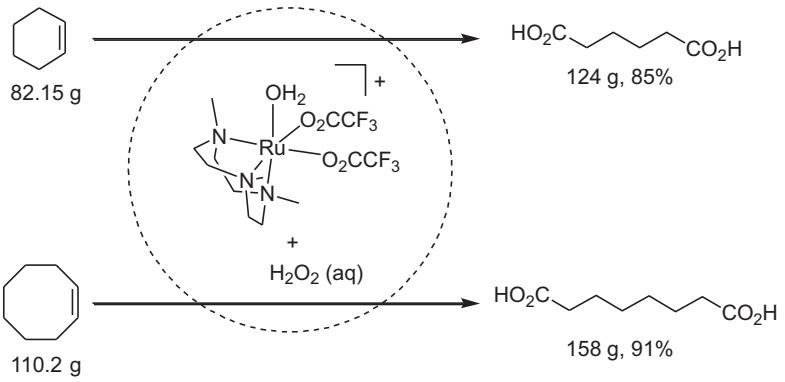

Scheme 23.

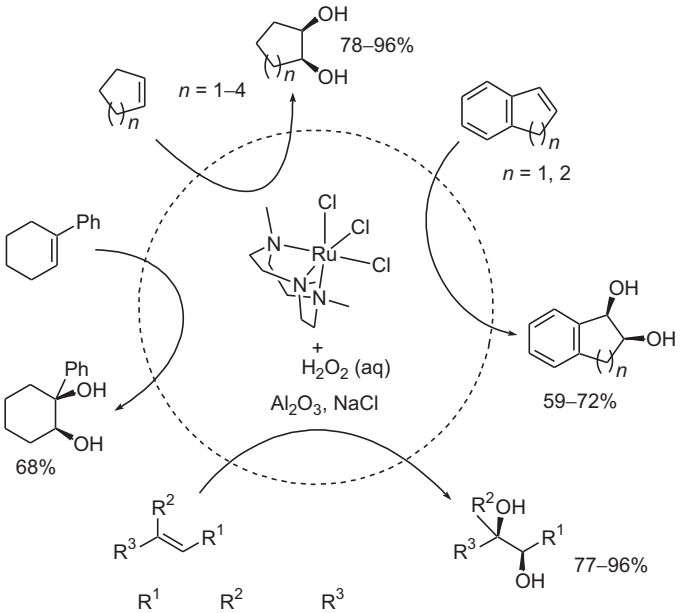

R^1	R^2	R^3
H	H	Ph, *n*-Bu, *n*-C_9H_{19}
H	Me	Ph
n-Bu	H	*n*-Bu
Me	Ph	H
Me	H	Ph

Scheme 24.

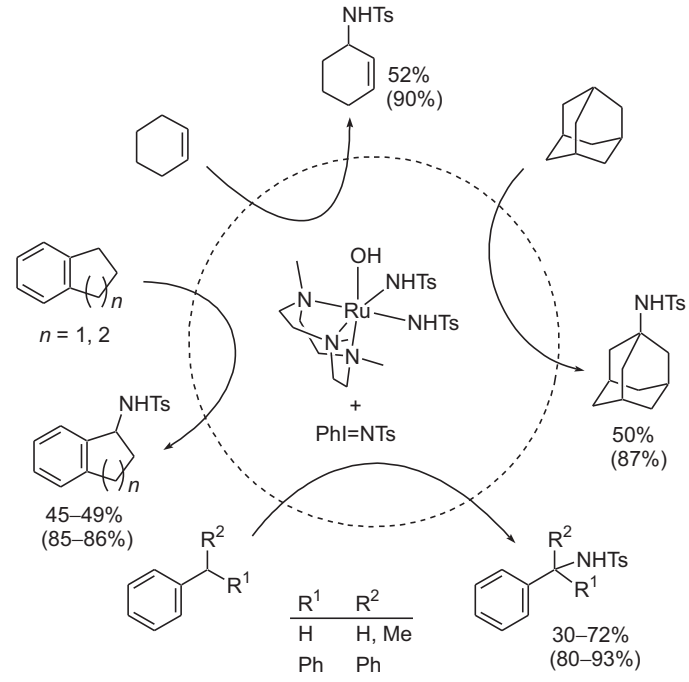

R^1	R^2
H	H, Me
Ph	Ph

(Yields in parentheses were obtained using $[Ru^{III}(Me_3tacn)(OH_2)(CF_3CO_2)_2]^+$ as catalyst.)

Scheme 26.

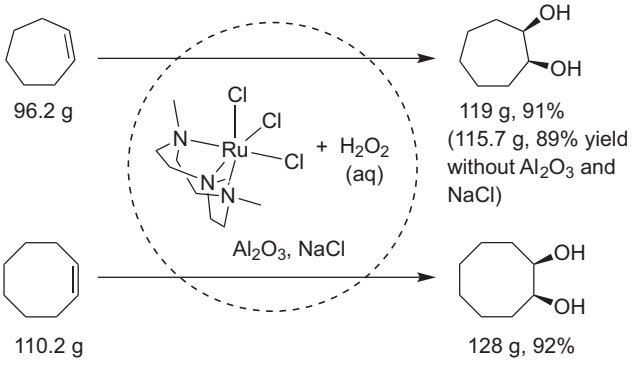

Scheme 25.

$[Ru^{II}(Me_3tacn)(NH_3)_3](PF_6)_2$ was found to catalyze aziridination of styrene in 1,2-dichloroethane at room temperature with substrate conversion of 25% and product yield of 90% after a reaction time of 72 h [55].

By employing $[Ru^{III}(Me_3tacn)(OH_2)(CF_3CO_2)_2]CF_3CO_2$ as catalyst, the amination of benzylic C–H bonds of ethylbenzene with "$PhI(OAc)_2 + RNH_2$" afforded various amines in 85–90% yields [54b] (Scheme 27, substrate conversion: 51–76%). This "$[Ru^{III}(Me_3tacn)(OH_2)(CF_3CO_2)_2]CF_3CO_2 + PhI(OAc)_2 + RNH_2$" protocol, together with similar protocol using manganese porphyrin catalyst [67], provides a convenient means for C–H bond amination, without the need to pre-isolate PhI=NR, a type of nitrogen source required in conventional amination of saturated C–H bonds catalyzed by metal complexes via imido or nitrene transfer reactions.

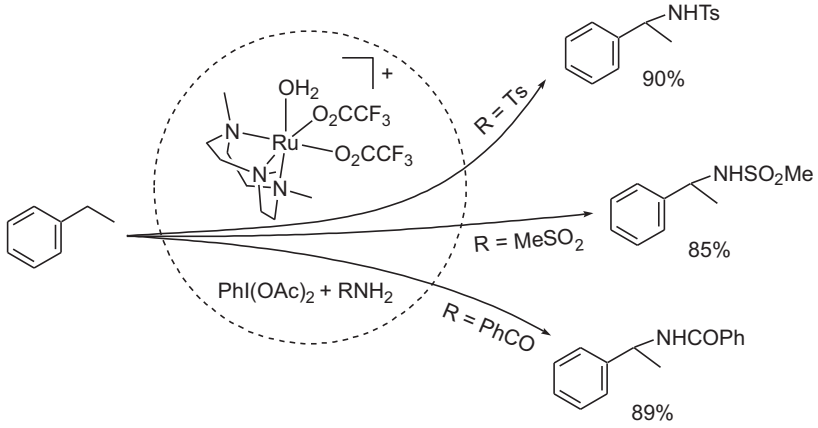

Scheme 27.

6. Conclusion

The tridentate Me_3tacn ligand system first synthesized by Wieghardt and co-workers provides a powerful support for metal–ligand multiple bonds, particularly M=O bonds which so far involve transition metals Ti, V, Mn, Mo, Ru, W, and Re in the isolated complexes. Especially interesting are the *cis*-dioxometal complexes supported by Me_3tacn, in which the two M=O bonds directed in a *cis* configuration by the facially coordinated Me_3tacn ligand are useful for selective vicinal *cis* functionalization of hydrocarbons such as *cis*-dihydroxylation of alkenes. Ruthenium is hitherto the only transition metal that forms a Me_3tacn-supported isolable *cis*-dioxo complex reactive toward alkene *cis*-dihydroxylation, despite the well documented catalytic activity of manganese and iron Me_3tacn complexes for oxidation reactions and the isolation of a number of *cis*-dioxo complexes of molybdenum, tungsten, and rhenium.

With its high oxidation capability, the structurally characterized *cis*-dioxoruthenium(VI) complex *cis*-$[Ru^{VI}(Me_3tacn)O_2(CF_3CO_2)]^+$ efficiently oxidizes alkynes and alkenes via a concerted [3+2] cycloaddition pathway, converting alkynes to α,β-diketones in up to 98% yield; the oxidation of alkenes affords either *cis*-diols in up to 85% yield or carboxylic acids in up to 91% yield via *cis*-dihydroxylation or C=C bond cleavage, respectively, depending on the reaction conditions. Monooxoruthenium(IV) complexes $[Ru^{IV}(Me_3tacn)O(N–N)]^{2+}$ (N–N = 2,2′-bipyridines), including the structurally characterized $[Ru^{IV}(Me_3tacn)O(bpy)](ClO_4)_2$, are competent oxidants for alkene epoxidation.

By using ruthenium Me_3tacn complex $[Ru^{III}(Me_3tacn)(OH_2)(CF_3CO_2)_2]^+$ as catalyst and *t*-BuOOH or aqueous H_2O_2 as terminal oxidant, a variety of catalytic oxidation reactions have been developed, ranging from alkene epoxidation to alkene *cis*-dihydroxylation, and from oxidation of alkanes, alcohols, aldehydes, and arenes to oxidative cleavage of C=C, C≡C, and C–C bonds, all with high selectivity. The oxidation of cycloalkenes to *cis*-diols, and the oxidation of cycloalkenes and primary alcohol to carboxylic acids, have been scaled up to 100 g scale, with the products being obtained in 85–92% yields.

The isolation of ruthenium-imido complexes supported by Me_3tacn remains a challenge, although metal Me_3tacn complexes bearing M=NR (M = Ti, Cr, Mo) have been isolated. Ruthenium-imido complexes are likely to be generated in the amination of saturated C–H bonds with PhI=NTs catalyzed by $[Ru^{III}(Me_3tacn)(OH_2)(CF_3CO_2)_2]^+$ or $[Ru^{III}(Me_3tacn)(NHTs)_2(OH)]$, as suggested by experiment and DFT calculation studies. $[Ru^{III}(Me_3tacn)(OH_2)(CF_3CO_2)_2]^+$ is also an efficient catalyst for C–H bond amination with "$PhI(OAc)_2 + RNH_2$", which affords various amines in 85–90% yields.

Acknowledgements

We acknowledge financial supports from the University Grant Council of Hong Kong SAR (Area of Excellence Scheme AoE/P-10/01) and the Hong Kong Research Grants Council (HKU 1/CRF/08 and HKU 7007/08P).

Appendix. Supplementary data

Supplementary data associated with this article can be found, in the online version, at doi:10.1016/j.ccr.2010.11.026.

References

[1] (a) L. Fabbrizzi, Comments Inorg. Chem. 4 (1985) 33;
(b) L. Fabbrizzi, M. Licchelli, L. Mosca, A. Poggi, Coord. Chem. Rev. 254 (2010) 1628.
[2] B. Bosnich, C.K. Poon, M.L. Tobe, Inorg. Chem. 4 (1965) 1102.
[3] C.-M. Che, V.W.-W. Yam, Adv. Inorg. Chem. 39 (1992) 233.
[4] J.-U. Rohde, J.-H. In, M.H. Lim, W.W. Brennessel, M.R. Bukowski, A. Stubna, E. Münck, W. Nam, L. Que Jr., Science 299 (2003) 1037.
[5] H. Koyama, T. Yoshino, Bull. Chem. Soc. Jpn. 45 (1972) 481.
[6] K. Wieghardt, P. Chaudhuri, B. Nuber, J. Weiss, Inorg. Chem. 21 (1982) 3086.
[7] (a) P. Chaudhuri, K. Wieghardt, Prog. Inorg. Chem. 35 (1987) 329;
(b) K. Wieghardt, Pure Appl. Chem. 60 (1988) 509;
(c) K.P. Wainwright, Coord. Chem. Rev. 166 (1997) 35.
[8] (a) K. Wieghardt, U. Bossek, D. Ventur, J. Weiss, J. Chem. Soc. Chem. Commun. (1985) 347;
(b) K. Wieghardt, U. Bossek, B. Nuber, J. Weiss, J. Bonvoisin, M. Corbella, S.E. Vitols, J.J. Girerd, J. Am. Chem. Soc. 110 (1988) 7398, and references therein.
[9] R. Hage, J.E. Iburg, J. Kerschner, J.H. Koek, E.L.M. Lempers, R.J. Martens, U.S. Racherla, S.W. Russell, T. Swarthoff, M.R.P. van Vliet, J.B. Warnaar, L. van der Wolf, B. Krijnen, Nature 369 (1994) 637.
[10] K.F. Sibbons, K. Shastri, M. Watkinson, Dalton Trans. (2006) 645.
[11] B. Mauerer, J. Crane, J. Schuler, K. Wieghardt, B. Nuber, Angew. Chem. Int. Ed. Engl. 32 (1993) 289.
[12] D.H. Jo, L. Que Jr., Angew. Chem. Int. Ed. 39 (2000) 4284.
[13] (a) E.Y. Tshuva, D. Lee, W. Bu, S.J. Lippard, J. Am. Chem. Soc. 124 (2002) 2416;
(b) R.F. Moreira, E.Y. Tshuva, S.J. Lippard, Inorg. Chem. 43 (2004) 4427.
[14] K. Wieghardt, G. Backes-Dahmann, B. Nuber, J. Weiss, Angew. Chem. Int. Ed. Engl. 24 (1985) 777.
[15] P. Schreiber, K. Wieghardt, B. Nuber, J. Weiss, Z. Anorg. Allg. Chem. 587 (1990) 174.
[16] W.-C. Cheng, W.-Y. Yu, K.-K. Cheung, C.-M. Che, J. Chem. Soc. Dalton Trans. (1994) 57.
[17] W.-C. Cheng, W.-Y. Yu, K.-K. Cheung, C.-M. Che, J. Chem. Soc. Chem. Commun. (1994) 1063.
[18] A. Niemann, U. Bossek, G. Haselhorst, K. Wieghardt, B. Nuber, Inorg. Chem. 35 (1996) 906.
[19] F.-W. Lee, M.C.-W. Chan, K.-K. Cheung, C.-M. Che, J. Organomet. Chem. 552 (1998) 255.
[20] M.C.-W. Chan, F.-W. Lee, K.-K. Cheung, C.-M. Che, J. Chem. Soc. Dalton Trans. (1999) 3197.
[21] (a) B.C. Gilbert, N.W.J. Kamp, J.R. Lindsay Smith, J. Oakes, J. Chem. Soc. Perkin Trans. 2 (1998) 1841;
(b) B.C. Gilbert, J.R. Lindsay Smith, A. Mairata, i. Payeras, J. Oakes, Org. Biomol. Chem. 2 (2004) 1176.
[22] T.H. Bennur, D. Srinivas, S. Sivasanker, V.G. Puranik, J. Mol. Catal. A-Chem. 219 (2004) 209.
[23] K.L. Klotz, L.M. Slominski, A.V. Hull, V.M. Gottsacker, R. Mas-Ballesté, L. Que Jr., J.A. Halfen, Chem. Commun. (2007) 2063.
[24] K.L. Klotz, L.M. Slominski, M.E. Riemer, J.A. Phillips, J.A. Halfen, Inorg. Chem. 48 (2009) 801.
[25] A. Bodner, P. Jeske, T. Weyhermüller, K. Wieghardt, E. Dubler, H. Schmalle, B. Nuber, Inorg. Chem. 31 (1992) 3737.
[26] P. Jeske, G. Haselhorst, T. Weyhermüller, K. Wieghardt, B. Nuber, Inorg. Chem. 33 (1994) 2462.
[27] (a) M. Köppen, G. Fresen, K. Wieghardt, R.M. Llusar, B. Nuber, J. Weiss, Inorg. Chem. 27 (1988) 721;
(b) D. Fiedler, O.S. Miljanić, E.J. Welch, Acta Crystallogr. E 58 (2002) m347.
[28] K.S. Bürger, G. Haselhorst, S. Stötzel, T. Weyhermüller, K. Wieghardt, B. Nuber, J. Chem. Soc. Dalton Trans. (1993) 1987.
[29] G. Backes-Dahmann, W. Herrmann, K. Wieghardt, J. Weiss, Inorg. Chem. 24 (1985) 485.
[30] D.V. Partyka, R.J. Staples, R.H. Holm, Inorg. Chem. 42 (2003) 7877.
[31] G. Barrado, L. Doerrer, M.L.H. Green, M.A. Leech, J. Chem. Soc. Dalton Trans. (1999) 1061.
[32] P.S. Roy, K. Wieghardt, Inorg. Chem. 26 (1987) 1885.
[33] W.-C. Cheng, W.-Y. Yu, J. Zhu, K.-K. Cheung, S.-M. Peng, C.-K. Poon, C.-M. Che, Inorg. Chim. Acta 242 (1996) 105.
[34] W.-Y. Yu, W.-H. Fung, J.-L. Zhu, K.-K. Cheung, K.-K. Ho, C.-M. Che, J. Chin. Chem. Soc. 46 (1999) 341.
[35] G. Backes-Dahmann, K. Wieghardt, Inorg. Chem. 24 (1985) 4049.
[36] R.R. Conry, J.M. Mayer, Inorg. Chem. 29 (1990) 4862.
[37] G. Böhm, K. Wieghardt, B. Nuber, J. Weiss, Inorg. Chem. 30 (1991) 3464.
[38] (a) W.A. Herrmann, P.W. Roesky, F.E. Kühn, W. Scherer, M. Kleine, Angew. Chem. Int. Ed. Engl. 32 (1993) 1714;
(b) W.A. Herrmann, P.W. Roesky, F.E. Kühn, M. Elison, G. Artus, W. Scherer, C.C. Romão, A. Lopes, J.-M. Basset, Inorg. Chem. 34 (1995) 4701.
[39] C.-M. Che, J.Y.K. Cheng, K.-K. Cheung, K.-Y. Wong, J. Chem. Soc. Dalton Trans. (1997) 2347.
[40] P.J. Wilson, A.J. Blake, P. Mountford, M. Schröder, J. Organomet. Chem. 600 (2000) 71.
[41] T.B. Parsons, N. Hazari, A.R. Cowley, J.C. Green, P. Mountford, Inorg. Chem. 44 (2005) 8442.
[42] S.-M. Yang, M.C.-W. Chan, K.-K. Cheung, C.-M. Che, S.-M. Peng, Organometallics 16 (1997) 2819.
[43] C.-Y. Wong, L.-M. Lai, C.-Y. Lam, N. Zhu, Organometallics 27 (2008) 5806.
[44] K. Meyer, J. Bendix, N. Metzler-Nolte, T. Weyhermüller, K. Wieghardt, J. Am. Chem. Soc. 120 (1998) 7260.
[45] W.-H. Fung, W.-Y. Yu, C.-M. Che, J. Org. Chem. 63 (1998) 7715.
[46] C.-M. Che, W.-Y. Yu, P.-M. Chan, W.-C. Cheng, S.-M. Peng, K.-C. Lau, W.-K. Li, J. Am. Chem. Soc. 122 (2000) 11380.
[47] W.-P. Yip, W.-Y. Yu, N. Zhu, C.-M. Che, J. Am. Chem. Soc. 127 (2005) 14239.
[48] W.-C. Cheng, W.-H. Fung, C.-M. Che, J. Mol. Catal. A-Chem. 113 (1996) 311.

[49] W.-H. Cheung, W.-Y. Yu, W.-P. Yip, N.-Y. Zhu, C.-M. Che, J. Org. Chem. 67 (2002) 7716.
[50] W.-H. Fung, W.-Y. Yu, C.-M. Che, J. Org. Chem. 63 (1998) 2873.
[51] C.-M. Che, W.-P. Yip, W.-Y. Yu, Chem. Asian J. 1 (2006) 453.
[52] W.-H. Cheung, W.-P. Yip, W.-Y. Yu, C.-M. Che, Can. J. Chem. 83 (2005) 521.
[53] W.-P. Yip, C.-M. Ho, N. Zhu, T.-C. Lau, C.-M. Che, Chem. Asian J. 3 (2008) 70.
[54] (a) S.-M. Au, S.-B. Zhang, W.-H. Fung, W.-Y. Yu, C.-M. Che, K.-K. Cheung, Chem. Commun. (1998) 2677;
(b) S.-M. Au, J.-S. Huang, C.-M. Che, W.-Y. Yu, J. Org. Chem. 65 (2000) 7858.
[55] K.-L. Yip, PhD Thesis, The University of Hong Kong, 2005.
[56] (a) P. Neubold, K. Wieghardt, B. Nuber, J. Weiss, Angew. Chem. Int. Ed. Engl. 27 (1988) 933;
(b) P. Neubold, K. Wieghardt, B. Nuber, J. Weiss, Inorg. Chem. 28 (1989) 459.
[57] R. Schneider, T. Weyhermüller, K. Wieghardt, B. Nuber, Inorg. Chem. 32 (1993) 4925.
[58] W.-C. Cheng, PhD Thesis, The University of Hong Kong, 1995.
[59] G.S.-M. Tong, E.L.-M. Wong, C.-M. Che, Chem. Eur. J. 14 (2008) 5495.
[60] P. Hummel, J.R. Winkler, H.B. Gray, Dalton Trans. (2006) 168.
[61] W.-H. Chiu, PhD Thesis, The University of Hong Kong, 1995.
[62] (a) W.R. Murphy Jr., K.J. Takeuchi, T.J. Meyer, J. Am. Chem. Soc. 104 (1982) 5817;
(b) W.R. Murphy Jr., K. Takeuchi, M.H. Barley, T.J. Meyer, Inorg. Chem. 25 (1986) 1041.
[63] S.-M. Au, PhD Thesis, The University of Hong Kong, 1999.
[64] J. Du Bois, C.S. Tomooka, J. Hong, E.M. Carreira, Acc. Chem. Res. 30 (1997) 364.
[65] D.A. Evans, M.M. Faul, M.T. Bilodeau, J. Am. Chem. Soc. 116 (1994) 2742.
[66] V.B. Romakh, B. Therrien, G. Labat, H. Stoekli-Evans, G.B. Shul'pin, G. Süss-Fink, Inorg. Chim. Acta 359 (2006) 3297.
[67] (a) X.-Q. Yu, J.-S. Huang, X.-G. Zhou, C.-M. Che, Org. Lett. 2 (2000) 2233;
(b) J.-L. Liang, J.-S. Huang, X.-Q. Yu, N. Zhu, C.-M. Che, Chem. Eur. J. 8 (2002) 1563.